Hydrodynamic Stability of Plane Couette and Poiseuille Flow

A Comparative Analysis

John Bowllan, Sabina Haque, Andrew Jenkins, and Ricardo Rosales-Mesta

Department of Mathematics, Middlebury College

Advisor: Professor Michaela Kubacki, PhD.

The authors made use of the following LaTeXtemplate to create this book:

The Legrand Orange Book
LaTeX Template
Version 2.3 (8/8/17)

This template has been downloaded from:
http://www.LaTeXTemplates.com

Original template author:
Mathias Legrand (legrand.mathias@gmail.com)

Submitted May 14, 2018

Hydrodynamic Stability of Plane Couette and Poiseuille Flow: A Comparative Analysis

John Bowllan, Sabina Haque, Andrew Jenkins,
and Ricardo Rosales-Mesta
Department of Mathematics, Middlebury College

Acknowledgments

We would like to express our deep gratitude to Professor Kubacki, our research supervisor, for her enthusiastic encouragement, guidance, and critiques of this research work.

We would also like to extend our thanks to the Mathematics Department at Middlebury College for their help in offering us the resources and space to conduct our research.

Contents

1 Introduction 7

2 Characterizing Couette-Poiseuille Flow 11
2.1 Introduction 11
2.2 Laminar and Turbulent Flow 12
2.3 The Navier-Stokes Equations 13
2.3.1 Derivation of the Continuity Equation 13
2.3.2 Derivation of the Momentum Equation 14
2.3.3 PDE Classification 16
2.4 Derivation of Couette-Poiseuille Flow Velocity Profile 17
2.5 Special Cases: Plane Poiseuille and Plane Couette Flow 19

3 The Orr-Sommerfeld Equation 21
3.1 Introduction 21
3.2 The Non-Dimensional Navier-Stokes Equations 22
3.3 Perturbed Flow 23
3.4 The Orr-Sommerfeld Equation 24

4 The Variational Formulation 29
4.1 Introduction 29
4.2 Physical Motivations Behind Use of Requisite Function Spaces 30
4.3 Inner Products and Norms 30
4.4 Variational Formulation 36
4.5 Existence and Uniqueness of the Solution 39

5 The Finite Element Method 43
5.1 The Weak Formulation and Motivation 43
5.2 Understanding the Basics 44
5.3 Properties, Boundary Conditions and Cea's Lemma 45
5.4 Working with the Weak Formulation 46
5.5 Couette and Poiseuille Flows 48

6 Conclusion 51

Bibliography 54

1. Introduction

To study fluid dynamics means to study a hearty fraction of the fundamental physical processes that exist in the observable universe. Researchers in fluid dynamics study the flows of liquids and gases, focusing on topics ranging from geophysical currents of the Earth's oceans, meteorological studies of the atmosphere, and forces acting on swimming bacteria [3]. As evidenced from these examples, the applications of fluid dynamics research not only span multiple scientific disciplines, but also prove relevant at vastly different size scales. In addition, research in aerodynamics and hydraulics has proven responsible for many developments in modern technology, such as designing jets and boats to withstand difficult wind or ocean conditions. [9]. Thus, fluid dynamics plays a pertinent role both in understanding the physics of world surrounding us and in developing technology that has become instrumental to our daily lives, making it a valuable and worthwhile field of study.

Within fluid dynamics research until the 1960's, there existed only two main areas of interest – theory and experiment [1]. However, despite yielding significant advancements in the field, both of these approaches can be hindered by inherent limitations. As a result, computational fluid dynamics (CFD) emerged as a third branch of research in the field, emphasizing the use of numerical methods [1]. As modern computers have exponentially increased their capacity to handle highly complex algorithms and large data sets, computational fluid dynamics has become more and more popular. Each of the three branches of fluid dynamics research wield different strengths, allowing them to work in tandem: theory provides mathematical rigor and motivations for experiments, experiments justify abstract theories with indelible physical proof, and computation assists with interpretation and analysis of results.

Indeed, the analytical and numerical approaches to fluid dynamics problems are two sides of a mathematical coin. From the mathematician's perspective, nothing is certain without proof; deriving general expressions provides more concrete insight than any situation-specific phenomena observed in experiments, and closed form solutions bring essential rigor to posing fluid dynamics problems. However, the power of analytical approaches comes at the cost of their abstraction. That is, the fluid dynamics problems for which we can derive closed-form solutions must be quite simplis-

tic. Where formalism comes up short, approximations can be made to fill in the mathematical gaps with "close enough" answers. At this stage, numerical approximation becomes especially important.

Using computational approximations as tools to approach previously unsolvable problems, mathematicians can easily visualize and work with extreme physical cases of fluid flow. Despite this advantage, numerical methods can be limited by error accumulation and lack of complexity when considering the physics of the problem. For example, many flows reach a state of deterministic chaos, making any degree of approximation diverge from exact solutions in the long term. As we return to theory for further insight, it will be important to keep in mind how analytical and numerical approaches bolster each other.

Any discussion of the mathematical theory behind fluid dynamics would be incomplete without consideration of the Navier-Stokes equations, the governing equations of fluid flow [2]. A more in-depth discussion of these concepts takes place in the next chapter. The idea of fluid turbulence becomes pertinent here, as a nonlinear term in the Navier-Stokes equations accounts for this poorly-behaved flow. This nonlinear term also comprises the reason why most Navier-Stokes problems are unsolvable, as most real-life fluids exhibit some degree of turbulent flow. Finding unique solutions to the Navier-Stokes equations is such a challenging feat that it is one of the seven Clay Millennium Problems, for which a one million dollar prize is awarded to anyone that can successfully solve them [1].

A natural question that arises is if certain fluids are more predetermined to transition into states of turbulence from more well-behaved flows. The phenomena described here refers to a fluid's stability, or how it reacts to the introduction of a disturbance in the flow. Stable fluids can withstand the introduction of such perturbations and will not exhibit any visible effect on the initial state of the system, whereas unstable flows may transition into states of turbulence in reaction [4]. Problems concerning hydrodynamic stability also require solutions to the Navier-Stokes equations, for which we will examine numerical methods that allow mathematicians to approach the problem.

A particularly powerful numerical method utilized in fluid dynamics research is the Finite Element Method. The Finite Element Method works by formulating the partial differential equation in question into a weak formulation, and subdividing its corresponding domain into small finite subdomains. It then performs the weak formulation on each finite domain, resulting in a local description of the equation. The method finishes by assembling all the finite elements, having transformed all the problem into a linear system to which more numerical approaches can be applied. What sets the Finite Element Method apart from other numerical approaches is its direct discretization of partial differential equations into a geometrically complex domain, which is typically a drawback for other numerical methods. In addition, its refinement processes increase the overall accuracy of the method. The sheer amount of computational power that this approach requires, however, becomes significant drawback to the Finite Element Method.

As evidenced by the discussion provided here, there exists a strong need for understanding fluid dynamics in simple physical scenarios and using them as a bridge to understand more complex problems. One such example is plane Couette-Poiseuille flow, which considers the flow of an incompressible viscous fluid in between two flat surfaces. Focusing on this type of fluid flow provides us the simplest physical scenario that exhibits complex behavior – it can be analyzed mathematically, but also can serve as a model for higher level problems. In addition, the use of simpler flows provides a useful template for readers to appreciate the various tools available in fluid dynamics and how engineers and mathematicians would attempt to solve related problems.

In this investigation, we seek to characterize the hydrodynamic stability of plane Couette-Poiseuille flows and its special cases (plane Couette and plane Poiseuille flow). We attempt to accomplish this task through analytical approaches and numerical methods. In particular, we apply the Navier-Stokes equations to these flows and discuss the physical discrepancies between the two scenarios and then derive the Orr-Sommerfeld equation to obtain mathematical tools necessary for stability analysis. We then move into the numerical methods phase of the project, where we will apply the Finite Element Methods to both plane Couette and plane Poiseuille flows. The purpose of this project is to utilize the simpler problem concerning plane Couette and Poiseuille flows as a lens to offer insight into how fluid dynamicists use different approaches to similar problems, to apply the findings of this work to more complex problems, and to develop a holistic analysis of hydrodynamic stability.

2. Characterizing Couette-Poiseuille Flow

2.1 Introduction

In this chapter, we begin by introducing some key principles requisite for understanding fluid dynamics as it relates to our project. We then delve into deriving the Navier-Stokes equations and discussing their classification as partial differential equations, making use of the heat equation as an example. Next, we use the Navier-Stokes equations to derive the velocity profile for plane Couette-Poiseuille flow. Finally, we will break down this derivation into two special cases, plane Couette and plane Poiseuille flow, and introduce some intuition into each flow's stability through consideration of the time-dependent case. Studies in hydrodynamic stability are intimately entangled with understanding the velocity field of a fluid, mathematically represented by $\mathbf{u}$. Thus, the purpose of this chapter is to demonstrate how analytical solutions to the Navier-Stokes equations, which yield a fluid's velocity profile, can assist with stating problems in hydrodynamic stability.

For the purposes of this project, we will focus our investigation on incompressible viscous fluids. A fluid is considered **incompressible** if it maintains constant density ρ within a **control volume** V, or an infinitesimal fluid element that moves with the flow velocity [3]. Flows with highly variable density fields are **compressible**, which is a characteristic property of gases. Incompressible flows are more commonly associated with liquids.

To define the second part of the phrase, a fluid's **viscosity** refers to an internal stress force acting parallel to the surface of the fluid, or a fluid's internal friction. Viscosity comes in two flavors – a fluid's dynamic viscosity μ represents its resistance to shearing flows, and its kinematic viscosity ν describes the ratio between μ and ρ. As a point of reference, consider a comparison between honey and water. The flow of honey is dramatically slower than that of water because honey has a much higher viscosity [1]. Conversely, non-viscous or **inviscid** fluids are rarely observed in nature. When certain materials (e.g. helium) are subjected to very low temperatures, they become zero viscosity-exhibiting superfluids [1].

As we discuss how to mathematically characterize incompressible viscous fluids in this chap-

ter, we intend to use their physical properties to introduce some intuition into their stability. For example, a fluid's **shear stress**, its flow velocity field at a single point $\mathbf{x}$, is represented as

$$\tau(\mathbf{x}) = \mu \nabla \mathbf{u}, \tag{2.1}$$

where the dynamic viscosity acts as a proportionality constant. It is of note that $\nabla \mathbf{u}$ is the fluid acceleration . Similarly, we can define the shear stress at the boundaries of the fluid as

$$\tau(y = 0) = \mu \nabla \mathbf{u}. \tag{2.2}$$

Because $\mathbf{u}$ often differs at a fluid's boundaries, particularly in the wall-bounded shear flows we will tackle later in the chapter, it is important to explicitly distinguish shear stress from wall shear stress.

Both shear stress and viscosity represent **internal forces** that act within the fluid as it tries to get out of its own way. As we narrow our focus onto particular flow scenarios, keeping the various effects of these internal forces in mind will prove essential.

2.2 Laminar and Turbulent Flow

When discussing fluids from a technical perspective, the need to articulate simple physical scenarios that can be modeled with mathematics becomes imperative. The scope of this project focuses on unidirectional flows moving through a channel. We describe fluids that move in uninterrupted parallel layers as **laminar flows**. To describe the mechanics that orchestrate laminar flow is a substantially simpler feat than to do so for the other extreme classification, **turbulent flows** [3]. Figure 2.1 depicts a visualization of the velocity profiles for laminar and turbulent flows in a closed channel of width h.

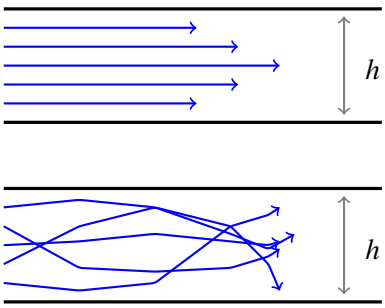

Figure 2.1: Visual representation of (a) laminar flow (b) turbulent flow in a 2D channel of width h

For laminar flows, as described above, the flow lines traverse the channel in parallel fashion. The layers, or *laminae*, of the fluid influence each other, with the flow at the center of the channel pushing the other layers forward. Common examples of naturally occurring laminar flows are blood flowing through capillaries or oil flowing through a tube. We assume the channel is solid so that any fluid at the boundary does not move. Mathematically, we describe this property as a **no-slip boundary condition** [3].

In contrast, irregular fluctuations characterize turbulent flows. The introduction of perturbations can disturb the fluid, which facilitates the conversion of laminar flows into turbulent flows. An example of this phenomenon is when smoke from a cigarette initially rises in a straight path but inevitably swirls and deviates from the original path or water coming out of a pipe and splattering in a sink [1].

We must note that when it comes to characterizing different flows, fluid dynamicists consider laminar flows the "best behaved" and turbulent flows the "worst behaved" categories. Many fluid flows exist in transitional states that lie in between laminar and turbulent. The transition a flow undergoes between laminar and turbulent states represents an incredibly complicated physical process [3]. Despite countless research efforts, this process has not been well-characterized or understood by mathematicians. A fluid's readiness to react to perturbations in its flow field, and in turn how quickly that fluid is able to transition from laminar to turbulent flows, defines its **stability** [4]. We will return to this connection between transition to turbulence and stability after we adopt the mathematical tools requisite for characterizing fluid flows.

2.3 The Navier-Stokes Equations

Mathematically, we describe the governing physical principles of fluid dynamics with the **Navier-Stokes equations** (Definition 2.3.3). These equations, as they apply to this project, articulate the conservation of momentum and the conservation of mass for incompressible viscous fluids.

In order to capture these fundamental physical phenomena, we must first define the concept of a material derivative of some quantity $\mathbf{X}$, where $\mathbf{X}$ represents a general vector with up to three components $\mathbf{X} = [u, v, w]$. In continuum mechanics, a **material derivative** is a mathematical description that reflects changes in time and space of a fluid element subject to a spacetime-dependent vector field. It has two components. The **local derivative** represents the time rate of change of some quantity at a fixed point in space, while the **convective derivative** represents the movement of a fluid element to another location in the vector field where the fluid's flow properties are spatially different. The general form of a material derivative takes the following form:

$$\frac{D}{Dt} = \frac{\partial}{\partial t} + (\mathbf{X} \cdot \nabla) \tag{2.3}$$

where $\frac{\partial}{\partial t}$ represents the local derivative and $(\mathbf{X} \cdot \nabla)$ is the convective derivative. Having a mathematical expression to describe spatiotemporal changes in a fluid's physical properties will prove essential to our efforts to derive the Navier-Stokes equations.

2.3.1 Derivation of the Continuity Equation

As we derive the conservation of mass, or the continuity equation, we can utilize the earlier discussion of the material derivative. We summarize the concept behind the conservation in Figure 2.2. Let $V = B(\mathbf{x}, \varepsilon)$, a ball with center $\mathbf{x}$ and radius ε, represent our infinitesimally small control volume as $\varepsilon \to 0$. As shown by the figure, we want to preserve the conservation of mass:

$$m_1 = m_2. \tag{2.4}$$

In other words, the material derivative of mass must equal zero:

$$\frac{Dm}{Dt} = 0. \tag{2.5}$$

Recall that density, ρ, equals $\frac{m}{V}$. We can now perform the following substitutions

$$\frac{D(\rho V)}{Dt} = V\frac{\partial \rho}{\partial t} + \rho\frac{DV}{Dt} = 0. \tag{2.6}$$

$$\frac{\partial \rho}{\partial t} + \rho\left(\frac{1}{V}\frac{DV}{Dt}\right) = 0. \tag{2.7}$$

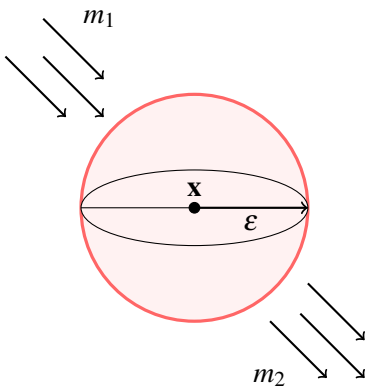

Figure 2.2: Geometric representation of net mass flow in and out of a control volume $V = B(\mathbf{x}$. Let m_1 represent net mass flow in and m_2 represent net mass flow out.

It can be shown with the Divergence Theorem that

$$\nabla \cdot \mathbf{u} = \frac{1}{V}\frac{DV}{Dt}[1]. \tag{2.8}$$

Thus, recognizing the convective derivative of $\mathbf{u}$ allows us to state

$$\frac{\partial \rho}{\partial t} + \rho(\nabla \cdot \mathbf{u}) = 0. \tag{2.9}$$

Since the focus of this work is incompressible flow, recall that ρ takes on a constant value. Thus, we have the conservation of mass for incompressible flow:

Definition 2.3.1 — Conservation of Mass for Incompressible Flow.

$$\nabla \cdot \mathbf{u} = 0 \tag{2.10}$$

2.3.2 Derivation of the Momentum Equation

The conservation of momentum is more colloquially referred to as Newton's second law of motion $\mathbf{F} = m\mathbf{a}$. We derive the momentum equations by expressing the terms $\mathbf{F}$, m, and $\mathbf{a}$ as they apply to fluids. Let us begin our discussion of the fluid forces $\mathbf{F}$ on an infinitesimal fluid element by considering Figure 2.3. Visualized in Figure 2.3 are the internal, or **surface forces** acting on an infinitesimally small fluid element of volume dV at some point in time. τ_{ii} represents a normal force acting on the fluid, while τ_{ij} represents a shearing force in direction j on the plane with $\mathbf{n}$ in the i direction. Fluids can also be subject to external **body forces**, which we will represent as $\rho \mathbf{f} dV$. We can represent $\mathbf{F_x}$ as follows:

$$\mathbf{F} = \mathbf{f_{body}} + \mathbf{f_{surface}}. \tag{2.11}$$

Let us begin by considering only the forces in the x direction:

$$\begin{aligned}\mathbf{F_x} =_x dV + \left(\tau_{xx} + \frac{\partial \tau_{xx}}{\partial x}dx - p - \frac{\partial p}{\partial x}dx\right)dydz + (-\tau_{xx} + p)dydz \\ + (-\tau_{zx})dxdy + \left(\tau_{zx} + \frac{\partial \tau_{zx}}{\partial z}dz\right)dxdy \\ + \left(\tau_{yx} + \frac{\partial \tau_{yx}}{\partial y}dy\right)dxdz + (-\tau_{yx}dxdz).\end{aligned} \tag{2.12}$$

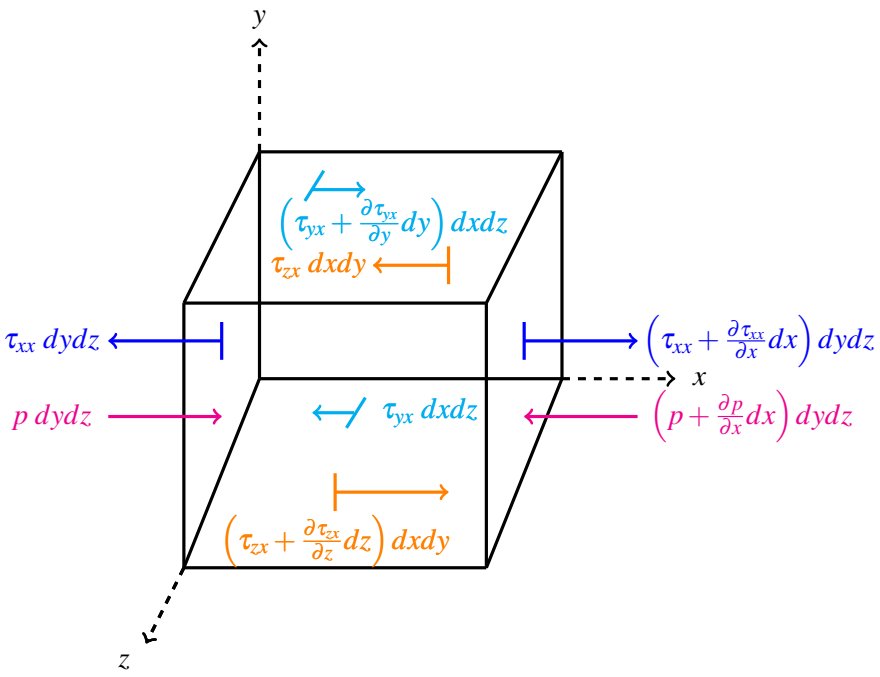

Figure 2.3: An infinitesimally small, moving fluid element. Only the forces in the x direction are shown. Adapted from [1].

Cancelling terms and applying the same logic to the y and z directions allows us to simplify this expression to

$$\mathbf{F} = \left(\rho \begin{bmatrix} f_x \\ f_y \\ f_z \end{bmatrix} + \nabla \cdot \begin{bmatrix} \tau_{xx} & \tau_{xy} & \tau_{xz} \\ \tau_{yx} & \tau_{yy} & \tau_{yz} \\ \tau_{zx} & \tau_{zy} & \tau_{zz} \end{bmatrix} - \begin{bmatrix} \frac{\partial p}{\partial x} \\ \frac{\partial p}{\partial y} \\ \frac{\partial p}{\partial z} \end{bmatrix} \right) dV, \tag{2.13}$$

or, more simply,

$$\mathbf{F} = (\rho \mathbf{f} + \nabla \cdot \tau - \nabla p)\, dV. \tag{2.14}$$

Now, let us consider how to rewrite the right-hand side of Newton's second law. The fluid's acceleration $\mathbf{a}$ is represented as the material derivative of its velocity $\frac{D\mathbf{V}}{dt} = \frac{\partial \mathbf{u}}{\partial t} + (\mathbf{u} \cdot \nabla)\mathbf{u}$. Mass m, as we know from the previous section, be represented as the product of the fluid density and volume, $m = \rho dV$. So, we have

$$\mathbf{F} = \rho dV \left(\frac{D\mathbf{V}}{dt} = \frac{\partial \mathbf{u}}{\partial t} + (\mathbf{u} \cdot \nabla)\mathbf{u} \right). \tag{2.15}$$

Equating the two expressions for $\mathbf{F}$ yields

$$\rho \left(\frac{D\mathbf{V}}{dt} = \frac{\partial \mathbf{u}}{\partial t} + (\mathbf{u} \cdot \nabla)\mathbf{u} \right) = \rho \mathbf{f} + \nabla \cdot \tau - \nabla p. \tag{2.16}$$

In the cases we intend to consider for our project, we can neglect body forces for fluids bounded by the plates of a 2D channel. Let us consider the term $\nabla \cdot \tau$, which is called the **Cauchy stress vector**. For the fluids in our project, the stress is proportional to the rate of deformation [1]

$$\tau \propto \mu \frac{\partial u}{\partial y}. \tag{2.17}$$

As we take advantage of this linear relationship and apply the Divergence Theorem, we obtain the following [1]:

$$\nabla \cdot \tau = \mu \Delta \mathbf{u}, \tag{2.18}$$

where $\Delta \mathbf{u}$ represents the Laplacian of the velocity. For simplicity of notation, we rescale the momentum equation by ρ, yielding our equation for the conservation of momentum.

Definition 2.3.2 — Conservation of Momentum for Incompressible Flow.

$$\frac{\partial \mathbf{u}}{\partial t} + (\mathbf{u} \cdot \nabla)\mathbf{u} = \nu \Delta \mathbf{u} - \frac{\nabla p}{\rho} \tag{2.19}$$

2.3.3 PDE Classification

Based off of the physical interpretations given for the conservation of momentum and mass in fluid mechanics, let us formally state the Navier-Stokes equations:

Definition 2.3.3 — Navier-Stokes Equations for Incompressible Viscous Fluids.

$$\frac{\partial \mathbf{u}}{\partial t} + (\mathbf{u} \cdot \nabla)\mathbf{u} = \nu \Delta \mathbf{u} - \frac{\nabla p}{\rho} \qquad \text{(Momentum Equation)}$$

$$\nabla \cdot \mathbf{u} = 0 \qquad \text{(Continuity Equation)}$$

Using these equations, we can investigate the governing physical principles as they apply to fluids in varying scenarios. There are several features here that are important to note. First, the convective derivative of velocity, $(\mathbf{u} \cdot \nabla)\mathbf{u}$, is a non-linear term. For laminar flows, this term is negligible, but it begins to matter once turbulence is considered. As mentioned previously, this nonlinear term also accounts for why most Navier-Stokes problems are almost impossible to solve. Also, recall that the kinematic viscosity ν is the quotient of the dynamic viscosity μ and the fluid density ρ. The right-hand side of the equations represents the balance between viscous and pressue-based internal forces within the fluid. In the next chapter, we will define a quantity called the **Reynolds number** that will allow us to quantify the stabilizing or destabilizing effect these forces have on a fluid.

The Navier-Stokes equations can be classified as either **parabolic** or **elliptic** partial differential equations [5]. Steady viscous flows yield elliptic equations, while the equations for unsteady viscous flows are parabolic in nature. There exists a third class of PDEs, **hyperbolic** equations, but this only applies to inviscid fluids and is thus irrelevant to the purposes of our project. Each class of PDEs demonstrates different mathematical behavior, which carries into the physical behavior of flow fields as well [1]. In order to observe these changes in mathematical behavior, we must utilize the **characteristic curves** that correspond to each PDE.

We express linear, second order PDEs, such as the **heat equation**, by writing an expression for their corresponding characteristic curve as follows:

$$aw_{xx} + bw_{xy} + cw_{yy} + dw_x + ew_y + fw = g, \tag{2.20}$$

for some function $w(x,y,z,t)$ and where subscripts represent the variable with respect to which partial differentiation occurs. Let us consider how one might classify the nonhomogeneous heat

equation,

$$w_t - \Delta w = -\frac{dp}{dx}. \tag{2.21}$$

Here, we can see that $a = -1$, and $b = c = 0$. To classify PDEs, we must consider the sign of the discriminant $b^2 - 4ac$. In this case, since the discriminant for the heat equation is 0, we can state that it is a parabolic differential equation. Equations for which $b^2 - 4ac < 0$ are elliptic in nature.

With regards to the Navier-Stokes equations, elliptic equations are much more difficult to solve than parabolic equations, as they do not yield any characteristic curves [5]. This mathematical difficulty results from the time-dependence of parabolic PDEs, which means that disturbances only affect the fluid at a later time. Disturbances in fluids with elliptic PDEs propagate throughout the entire fluid in all directions. Understanding this discrepancy between viscous fluids will lend to our further investigations of hydrodynamic stability.

2.4 Derivation of Couette-Poiseuille Flow Velocity Profile

Here, we seek to solve the Navier-Stokes equations of continuity and momentum for the conditions of Couette-Poiseuille flow. **Couette-Poiseuille flow** is a specific physical scenario describing a fluid traversing a two-dimensional channel. The top plate is moving with velocity U and the fluid is also driven by a constant pressure gradient $\frac{dp}{dx} = G$.

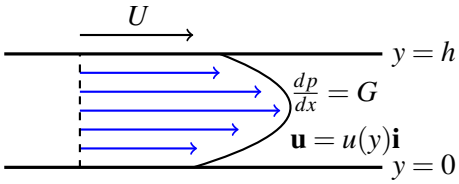

Figure 2.4: Couette-Poiseuille flow in a 2D channel of width h

Let us define the specific conditions for Couette-Poiseuille flow, where $\mathbf{u} = [u(x,y,z), v(x,y,z), w(x,y,z)]$:

$$v = w = 0 \tag{2.22}$$

$$u = u(y) \tag{2.23}$$

$$p = p(x). \tag{2.24}$$

So, we consider a velocity field, which is a function of y, that only moves in the x-direction. To explain why we describe the velocity field as a function of y, picture the dashed line in Figure 1.2 as the y-axis and the lower plate as the x-axis. The fluid velocity changes with respect to the y-axis, not the x-axis. It follows that pressure acts perpendicular to the fluid surface, leading to its definition as a function of x. For this work, we focus on the steady-state of stationary case (meaning $\frac{\partial u}{\partial t} = 0$). The application of these conditions translates to the following:

$$\mathbf{u} = [u(y), 0, 0] \tag{2.25}$$

$$\frac{\partial \mathbf{u}}{\partial t} = \frac{\partial u}{\partial t} = 0 \tag{2.26}$$

$$(\mathbf{u} \cdot \nabla)\,\mathbf{u} = \frac{\partial u(y)}{\partial x}\mathbf{u} = 0 \tag{2.27}$$

$$\frac{\partial p}{\partial x} = \frac{dp}{dx}. \tag{2.28}$$

Thus, the Navier-Stokes equations reduce to

Definition 2.4.1 — Reduced Momentum Equation for Couette-Poiseuille flow.

$$\frac{dp}{dx} = \mu \frac{\partial^2 u}{\partial y^2}. \tag{2.29}$$

We now have a second order differential equation which, when solved for, will yield the velocity profile for Couette-Poiseuille flow. Because this equation describes steady viscous flow, the resulting equation is elliptic, which means that disturbances in the interior of the fluid affect the fluid at all locations. This expression represents the balance between the viscous shear forces (represented by μ) and the constant applied pressure gradient $\frac{dp}{dx} = G$ acting on the fluid simultaneously.

To find a solution for the velocity profile, $u(y)$, we first integrate the reduced momentum equation twice with respect to y after setting it equal to 0. Let C and D represent the resulting integration constants:

$$\int \mu \frac{\partial^2 u}{\partial y^2} - \frac{dp}{dx} dy = \mu \frac{\partial u}{\partial y} - y \frac{dp}{dx} + C \tag{2.30}$$

$$\int \mu \frac{\partial u}{\partial y} - \frac{y^2}{2} \frac{dp}{dx} + C dy = \mu u - \frac{y^2}{2} \frac{dp}{dx} + Cy + D. \tag{2.31}$$

$$u(y) = \frac{y^2}{2\mu} \frac{dp}{dx} - \frac{Cy}{\mu} - \frac{D}{\mu}. \tag{2.32}$$

This represents a family of velocity profiles. To specify a particular velocity profile, we must enforce the boundary conditions at $y = 0$ and $y = h$. For this particular flow, since our velocity is specified explicitly on the boundary, we have the **homogeneous Dirichlet boundary condition** of $u(-L) = 0$ and $u(L) = U$, which in turn allows us to solve for constants C and D. Let us begin with the boundary condition $u(0) = 0$:

$$0 = \frac{0^2}{2\mu} \frac{dp}{dx} - C \cdot 0 - \frac{D}{\mu}, \tag{2.33}$$

$$D = 0. \tag{2.34}$$

Now, for the second boundary condition $u(h) = U$:

$$U = \frac{h^2}{2\mu} \frac{dp}{dx} - \frac{Ch}{\mu}, \tag{2.35}$$

$$C = \frac{h}{2} \frac{dp}{dx} - \mu \frac{U}{h}. \tag{2.36}$$

Plugging these solutions back into the original equation yields:

$$u(y) = \frac{y^2}{2\mu}\frac{dp}{dx} - \frac{y}{\mu}\left(\frac{h}{2}\frac{dp}{dx} - \mu\frac{U}{h}\right). \tag{2.37}$$

By simplifying, we obtain the velocity profile for combined Couette-Pouseuille flow:

Definition 2.4.2 — Velocity Profile for Couette-Pouseuille flow.

$$u(y) = -\frac{y}{2\mu}\frac{dp}{dx}(h-y) + \frac{U}{h}y \tag{2.38}$$

2.5 Special Cases: Plane Poiseuille and Plane Couette Flow

The combined Poiseuille-Couette flow case assumes that two physical forces drive the flow of the fluid: a laterally moving upper plate with velocity U and a constant applied pressure gradient $\frac{dp}{dx} > 0$. Assuming no applied pressure gradient gives us Couette flow, where the movement of the upper plate drives the flow of the fluid.

Definition 2.5.1 — Plane Couette Flow. Plane Couette flow is the special case of combined Couette-Poiseuille flow where the fluid is driven by the velocity of the moving upper plate U and the applied pressure gradient is nonexistent. These conditions correspond to the following *linear* velocity profile.

$$u(y) = \frac{U}{h}y \tag{2.39}$$

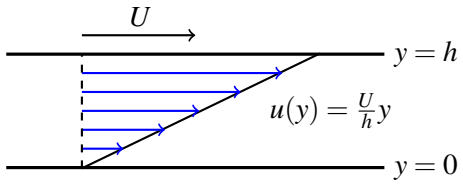

Figure 2.5: Couette flow in a 2D channel of width h

Physical examples of Couette flow include wind-driven flow in a body of water, where the wind represents a moving plate and the water represents a steady plate, or rubbing sunscreen on your arm. The opposite case, Poiseuille flow, assumes that the upper plate is not moving and that the fluid flow is driven solely by the constant applied pressure gradient. A key example of plane Poiseuille flow is squeezing toothpase out of a tube.

Definition 2.5.2 — Plane Poiseuille Flow. Plane Poiseuille flow is the special case of combined Couette-Poiseuille flow where the fluid is driven by a constant applied pressure gradient $\frac{dp}{dx} = G > 0$ and the upper plate is stationary. These conditions correspond to the following *quadratic*

velocity profile.

$$u(y) = -\frac{y}{2\mu}\frac{dp}{dx}(h-y) \tag{2.40}$$

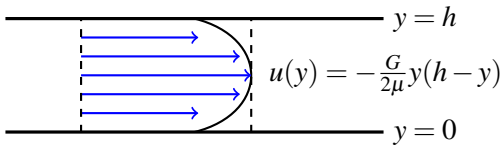

Figure 2.6: Poiseuille flow in a 2D channel of width h

Recall our earlier discussion of internal forces such as shear stress at the beginning of the chapter. Shear stress represents a physical discrepancy that arises between plane Couette and plane Poiseuille flow. In plane Couette flow, shear forces drive the fluid motion as initiated by the moving plate. In contrast, the layers at the center of Poiseuille flow pulls the peripheral layers along with it, as can be witnessed from its quadratic velocity profile.

Differentiating the velocity profile for plane Couette flow (2.5.1) and multiplying by μ results in the shear stress for plane Couette flow:

$$\tau_c = \mu\frac{U}{h}. \tag{2.41}$$

Note that the shear stress for plane Couette flow, which is equal to the wall shear stress $\tau_{c/wall}$, is constant throughout the flow domain. Applying the same process to plane Poiseuille flow yields the following result, replacing $\frac{dp}{dx}$ with a constant value $G > 0$:

$$\tau_p = -G(\frac{h}{2} - y). \tag{2.42}$$

Here, since the shear stress is dependent on the position y, the wall shear stress for Poiseuille flow is not equal to the shear stress of the fluid, which is

$$\tau_{p/wall} = -G(\frac{h}{2}). \tag{2.43}$$

Understanding the mathematical nature of fluid dynamics proves indispensable for our purpose in stating problems in hydrodynamic stability. Comparing the shear stresses between Couette and Poiseuille flow reveals that the differences in conditions results in differences between the internal forces. These internal forces can be used as means to investigate the potential effects that various perturbations might have on the stability of each flow. Another key aspect to note is the effect balance between dampening viscous and agitating pressure forces may have on fluid stability. Finally, characterizing the mechanisms through which disturbances propagate through the fluid based on their PDE classification yields a strong foundation for understanding fluid stability.

3. The Orr-Sommerfeld Equation

3.1 Introduction

The Orr-Sommerfeld equation, named for the mathematicians who first described it circa 1907 is the equation governing the linear stability of viscous plane parallel flow. It is analogous to the Raleigh Stability equation for inviscid fluids, although this result was published some thirty years prior. [4] Additionally, the Orr-Sommerfeld equation only describes a two dimensional flow, although in 1933 Squire showed that the two dimensional problem was sufficient to find a lower bound on the parameters leading to instability.[15] This makes the Orr-Sommerfeld equation a powerful tool for analyzing general linear stability.

In this chapter we derive this equation. As shown in the previous section, many of the basic properties of plane parallel flow can be described directly from the Navier-Stokes equations. In fact all viscous plane parallel flows can be expressed as a linear combination of the Couette and Poisseuille special cases. This behavior is remarkably simple.

In practice however, the scenario modelled by plane parallel flow is never in the perfect equilibrium state of Couette-Poisseuille flow. A slight rattle or an irregularity in laboratory equipment could create small nonlaminar disturbances in the flow. If this causes our flow to totally transition out of the laminar regime, then Couette-Poisseuille flow is not a particularly accurate model of nature. Thus, the question of stability arises: If a small change is made to the flow, how do these effects propagate? Do they die off or do they grow to the point where our flow transitions out of a laminar state and toward turbulence?

The stability analysis given here relies on linearizing the equations of motion so that our perturbation may be expressed as a superposition of normal modes, with each of these modes having a particular stability condition. The Orr-Sommerfeld Equation, which encodes the permissible parameters in a given mode, is derived from this linearized equation. Along the way, we discuss the significance of the Reynold's number and prove Squire's theorem, a result which reduces our three dimensional stability problem to a more manageable two dimensions.

3.2 The Non-Dimensional Navier-Stokes Equations

We begin by expressing the Navier-Stokes equations in terms of non-dimensional variables. Non-dimesionalization allows us to rescale the problem such that the classes of flows with similar behavior due to their scale can be considered as single cases. For example, we see that dimensional and dimensionless continuity equations will be identical, meaning this equation has the same behavior regardless of the velocity profile and channel width. More subtly, we will see how this process allows us to consolidate the dimensional terms of the momentum equation into a single constant. In particular, this constant encodes how much the viscosity of the fluid impacts the flow, taking into account the dimensional constraints of the channel.

We introduce a characteristic length scale, L, and velocity scale, V, equal to the half channel width and maximum value of the velocity profile, respectively, which we think of as constant conversion factors between our dimensional and dimensionless variables. Let dimensional variables be denoted with a bar. From these scales we define

$$\frac{\overline{\mathbf{u}}}{V} = \mathbf{u}, \tag{3.1}$$

$$\frac{\overline{\mathbf{x}}}{L} = \mathbf{x}, \tag{3.2}$$

$$\frac{\bar{t}}{L/V} = t. \tag{3.3}$$

As our fluid is incompressible, and thus ρ is constant, the pressure can also be expressed in terms of these characteristic scales:

$$\frac{\bar{p}L}{\rho V^2} = p. \tag{3.4}$$

However, our equation also involves taking derivatives of these variables with respect to a dimensional variable. The ∇ operator has three components, each corresponding to a spatial partial derivative. Thus, ∇ has units of 1/L. We therefore define the dimensionless operators $\overline{\nabla}$ and $\overline{\Delta}$ as follows

$$\overline{\nabla} L = \nabla, \tag{3.5}$$

$$\overline{\Delta} L^2 = \Delta \tag{3.6}$$

where the dimension of Δ follows from $\Delta = \nabla \cdot \nabla$.

These variables can be substituted into the Navier-Stokes Equations, neglecting body forces as no electric or gravitational field is present. This yields the equations

$$\rho \frac{\partial uV}{\partial t(L/V)} + \rho(uV \cdot \frac{\nabla}{L})uV = -\frac{\nabla}{L}(\rho V^2 p) + \mu(\Delta/L^2)uV, \tag{3.7}$$

$$\rho(\nabla \cdot uV) = 0. \tag{3.8}$$

For the continuity equation, we may divide out our dimensional constants to express our equation only in terms of dimensionless variables. In the momentum equation we divide by $\rho V^2/L$ so only the ultimate term has a coefficient not equal to unity. For convenience, we define a new quantity that is the reciprocal of this coefficient.

Definition 3.2.1 — Reynold's Number. The Reynold's number is defined in terms of the characteristic parameters such that

$$Re = \frac{\rho V L}{\mu} \tag{3.9}$$

Now the Navier-Stokes Equations take the form

Definition 3.2.2 — Non-dimensional Navier-Stokes Equations.

$$\frac{\partial u}{\partial t} + (u \cdot \nabla)u = -\nabla p + \frac{1}{Re}\Delta u \tag{3.10}$$

$$\nabla \cdot u = 0 \tag{3.11}$$

The Reynold's number was first introduced by Osbourne Reynold's in 1888 in the study of stability of pipe Poisseuille flow [4]. Reynold's insight was that flows with this same Reynold's number were dynamically equivalent, and thus the existence of stability would also be entirely determined by this value. In fact, Reynold's showed that after Re exceeded a certain value, the *critical Reynold's number*, the flow would transition to turbulence. This notion aligns well with intuition. A fluid that is highly viscous in comparison to its length and time scales, and thus has low Reynold's number, is difficult to disturb to the point that it turbulent phenomenon like vorteces begin to form. An example of this kind of system would be honey flowing through a tube. Conversely, we see turbulence arise in systems with low viscosity in comparison to their length scales, like a turbulent river.

With this new form of the Navier-Stokes equations at our disposal, we no longer have to separately consider how physical constraints, the general flow behavior, and the viscosity each affect the stability of the flow. Instead, we have a single new parameter which characterizes the dynamic behavior of the system. This significantly simplifies further analysis; instead of considering what sets of constraints create instability, we need only consider for which values of Re the flow is stable. We will see in the following section how the Reynold's number is related to the stability of a perturbation.

3.3 Perturbed Flow

Thus far we have nondimensionalized the Navier-Stokes equations. In order to study the stability of flows obeying this equation, we add a small perturbation **u'** and p' to the basic flow with appropriate nondimensionalization which may depend on all spatial and temporal variables. This perturbation may be thought of a slight shake or deformation of the velocity profile at a given time. As this perturbation is small, we ignore higher order terms to arrive at the linearized Navier-Stokes equations. This equation has the normally quadratic convective term replaced with a linear term. While this only approximates the behavior in terms of the perturbed flow, it allows for explicit solutions for the perturbation which will be critical in the stability analysis.

Definition 3.3.1 — Perturbed flow. The perturbed flow takes the form

$$\mathbf{u}_{new} = u\hat{\imath} + \mathbf{u}', \quad p_{new} = p + p' \tag{3.12}$$

where u is the basic flow

We want this new flow to be considered stable if the perturbation does not substantially impact the general behavior of the original flow. If the perturbation is damped out with time, the general behavior will roughly be the same as the underlying flow. This leads us to a formal definition of stability.

Definition 3.3.2 — Stability of a Flow. A given flow u is **stable** if the magnitude of the perturbed flow $\mathbf{u}_{new}$ remains finite as t $\longrightarrow \infty$

We thus proceed in analyzing the behavior of $\mathbf{u}_{new}$, seeking conditions for which instability ensues. Substituting $\mathbf{u}_{new}$ and p_{new} into the non-dimensionalized momentum and continuity equations gives

$$\frac{\partial u\hat{\imath}+\mathbf{u}'}{\partial t}+((u\hat{\imath}+\mathbf{u}')\cdot\nabla)(u\hat{\imath}+\mathbf{u}')=-\nabla(p+p')+\frac{1}{Re}\Delta(u\hat{\imath}+\mathbf{u}'), \tag{3.13}$$

$$\nabla\cdot(u\hat{\imath}+\mathbf{u}')=0. \tag{3.14}$$

As p is constant and the basic flow is divergence free, our U and p terms vanish in the right hand side of (2.10). This leaves

$$\frac{\partial \mathbf{u}'}{\partial t}+((u\hat{\imath}+\mathbf{u}')\cdot\nabla)(u\hat{\imath}+\mathbf{u}')=-\nabla p'+\frac{1}{Re}\Delta\mathbf{u}', \tag{3.15}$$

$$\nabla\cdot\mathbf{u}'=0. \tag{3.16}$$

The nonlinear term in this equation presents a serious roadblock for finding closed form solutions. However $|\mathbf{u}'| << 1$, so we may approximate by assuming terms quadratic in our disturbance are negligible. This simplifies our equation to the following.

$$\frac{\partial \mathbf{u}'}{\partial t}+(u\hat{\imath}\cdot\nabla)(u\hat{\imath}+\mathbf{u}')+(\mathbf{u}'\cdot\nabla)u\hat{\imath}=-\nabla p'+\frac{1}{Re}\Delta\mathbf{u}', \tag{3.17}$$

$$\nabla\cdot\mathbf{u}'=0. \tag{3.18}$$

In Couette-Poisseuille flow, the flow is in the x-direction, and thus only the x-component of the former term of the convective derivative does not cancel. In the latter term, we have a derivative of u, and as the basic flow only depends on y, only the y derivative in the x-direction is non-zero. We thus reach the fully simplified linearized equations of motion.

$$\frac{\partial \mathbf{u}'}{\partial t}+u\frac{\partial \mathbf{u}'}{\partial x}+\mathbf{u}'_y\frac{\partial u}{\partial y}\hat{\imath}=-\nabla p'+\frac{1}{Re}\Delta\mathbf{u}', \tag{3.19}$$

$$\nabla\cdot\mathbf{u}'=0. \tag{3.20}$$

Now that our equation of motion is linear, we may consider general closed form solutions, and proceed with an analysis of the conditions permitting stability.

3.4 The Orr-Sommerfeld Equation

With an equation of motion for our perturbation, we can now infer the conditions characterizing its qualitative behavior. First we note that all coefficients in the linearized equations of motion at most depend on y. This implies that solutions which are exponential in our remaining variables, namely x, z, and t, are permitted by the equations of motion.[4] We thus consider our solution as a superposition of modes, summed over the spectra of wave numbers present in our solution.

$$\mathbf{u}'=\sum_{\alpha}\sum_{\beta}\sum_{c}\hat{\mathbf{u}}(y,\alpha,\beta,c)e^{i(\alpha x+\beta y-\alpha ct)},$$

$$p'=\sum_{\alpha}\sum_{\beta}\sum_{c}\hat{p}(y,\alpha,\beta,c)e^{i(\alpha x+\beta y-\alpha ct)}.$$

Parallel shear flows are bounded in the y direction. As such, the y-component of any mode must remain bounded as our unconstrained spatial variables approach infinity, meaning α and β must be real. The wave speed c, however, may be complex. If Im(αc) is non-positive, then the magnitude of the mode remains bounded and is thus stable. If Im(αc) is positive, then the mode grows without bound.

If **u'** obeys the linearized equations of motion, so does any individual mode by linearity. This implies that the presence of any unstable mode in our sum results in an unstable flow. It is therefore sufficient for the purposes of stability analysis to consider a single arbitrary mode and determine the conditions which lead to positive imaginary components of c. Explicitly, our mode takes the form

$$\mathbf{u}'(\mathbf{x},t) = \hat{\mathbf{u}}(y)e^{i(\alpha x+\beta z-\alpha ct)}, \tag{3.21}$$

$$p'(\mathbf{x},t) = \hat{p}(y)e^{i(\alpha x+\beta z-\alpha ct)}. \tag{3.22}$$

Substituting these values into the linearized Navier-Stokes Equations gives

$$\begin{aligned}\frac{\partial}{\partial t}\hat{\mathbf{u}}(y)e^{i(\alpha x+\beta z-\alpha ct)} + u\frac{\partial}{\partial x}\hat{\mathbf{u}}(y)e^{i(\alpha x+\beta z-\alpha ct)} + \hat{u}_y e^{i(\alpha x+\beta z-\alpha ct)}\frac{\partial u}{\partial y}\hat{\imath} = \\ -\nabla\hat{p}e^{i(\alpha x+\beta z-\alpha ct)} + \frac{1}{Re}\Delta\hat{\mathbf{u}}(y)e^{i(\alpha x+\beta z-\alpha ct)}, \\ \nabla\cdot\hat{\mathbf{u}}(y)e^{i(\alpha x+\beta z-\alpha ct)} = 0.\end{aligned} \tag{3.23}$$

Consider the first term of the momentum equation. By the chain rule,

$$\frac{\partial}{\partial t}\hat{\mathbf{u}}(y)e^{i(\alpha x+\beta z-\alpha ct)} = \alpha ct\hat{\mathbf{u}}(y)e^{i(\alpha x+\beta z-\alpha ct)}. \tag{3.24}$$

We see that due to the exponential nature of the perturbation, each partial differentiation is equivalent to scaling by the wave number of the variable of the differentiation. As each term has the same exponential factor, we may also divide each of these out. This leaves

$$[\frac{\partial}{\partial y} - (\alpha^2+\beta^2) - i\alpha Re(U-c)]\hat{u}_x = Re\frac{\partial U}{\partial y}\hat{u}_y + i\alpha Re\hat{p}, \tag{3.25}$$

$$[\frac{\partial}{\partial y} - (\alpha^2+\beta^2) - i\alpha Re(U-c)]\hat{u}_y = Re\frac{\partial \hat{p}}{\partial y} \tag{3.26}$$

$$[\frac{\partial}{\partial y} - (\alpha^2+\beta^2) - i\alpha Re(U-c)]\hat{u}_z = i\beta Re\hat{p}, \tag{3.27}$$

$$i(\alpha\hat{u}_x + \beta\hat{u}_z) + \frac{\partial\hat{u}_y}{\partial y} = 0. \tag{3.28}$$

With the conditions that $\hat{\mathbf{u}}$ and $\hat{p}$ vanish at the boundaries of the channel.

These equations are significantly more complicated than the equations governing the velocity profile, largely because our flow is no longer unidirectional. However, our perturbation has roughly the same behavior in the x and z directions and we seek to exploit this symmetry in our analysis. We thus unite our x and z equations into the single linear combination α(3.25)+β(3.27)

$$[\frac{\partial}{\partial y} - (\alpha^2+\beta^2) - i\alpha Re(U-c)](\alpha\hat{u}_x + \beta\hat{u}_z) = \alpha Re\frac{\partial U}{\partial y}\hat{u}_y + i(\alpha^2+\beta^2)Re\hat{p}, \tag{3.29}$$

$$[\frac{\partial}{\partial y} - (\alpha^2+\beta^2) - i\alpha Re(U-c)]\hat{u}_y = Re\frac{\partial\hat{p}}{\partial y}, \tag{3.30}$$

$$i(\alpha\hat{u}_x + \beta\hat{u}_z) + \frac{\partial\hat{u}_y}{\partial y} = 0. \tag{3.31}$$

Notice now that the all instances of α and β, as well as $\hat{u}_x$ and $\hat{u}_z$ occur in pairs. This suggests that our three dimensional problem may be reduced to a simpler form. The following theorem was first described by Squire in 1933. [15]

Theorem 3.4.1 — Squire's Theorem. To find the critical Reynold's number it is sufficient to consider two dimensional disturbances.

Proof. We first define a transformation such that the x and z amplitudes of our perturbation can be considered as a single value.

Definition 3.4.1 — Squire Transformation. The Squire Transformation $\mathrm{T}(\alpha,\beta,c,Re,\hat{\mathbf{u}},\hat{p})$ is defined as follows

$$\begin{aligned}
\tilde{\alpha} &= T((\alpha^2+\beta^2)^{1/2}),\\
\tilde{\alpha}\tilde{u} &= T(\alpha\hat{u}_x+\beta\hat{u}_z),\\
\frac{\alpha\tilde{p}}{\tilde{\alpha}} &= T(\hat{p}),\\
\frac{\tilde{\alpha}\tilde{Re}}{\alpha} &= T(Re),\\
\tilde{u}_y &= T(\hat{u}_y),\\
\tilde{c} &= T(c).
\end{aligned}$$

The transformed equations of motion take the form

$$[\frac{\partial^2}{\partial y^2}-\tilde{\alpha}^2-i\tilde{\alpha}\tilde{Re}(u-c)]\tilde{\alpha}\tilde{u}_x = \tilde{\alpha}\tilde{Re}\frac{\partial U}{\partial y}\hat{u}_y + i\tilde{\alpha}^2 Re\hat{p}, \tag{3.32}$$

$$[\frac{\partial^2}{\partial y^2}-\tilde{\alpha}^2-i\tilde{\alpha}\tilde{Re}(u-c)]\tilde{u}_y = \frac{\alpha}{\tilde{\alpha}}\tilde{Re}\frac{\partial\tilde{p}}{\partial y}\frac{\tilde{\alpha}}{\alpha}, \tag{3.33}$$

$$i\tilde{\alpha}\tilde{u}_x+\frac{\partial\tilde{u}_y}{\partial y}=0, \tag{3.34}$$

with boundary conditions that $\mathrm{T}(\hat{\mathbf{u}})=\tilde{\mathbf{u}}=0$ at the boundaries of the channel.

Note that after dividing out multiples of $\tilde{\alpha}$, the transformed equations have the exact same form as our original, only with β and $\hat{u}_z$ set equal to zero. Our transformed problem is therefore equivalent to the three dimensional problem on this two dimensional slice of our original space.

What makes this transformation useful for stability analysis is the fact $\tilde{\alpha}\geq\alpha$, and thus $\tilde{Re}\leq Re$. Therefore if a flow transitions to instability at some critical Reynold's number in the three dimensional case, the flow in the two dimensional case must transition at an equal or lesser Reynold's number. ■

This transformation not only simplifies the rest of our calculation, but also shows a remarkable result in hydrodynamic stability: perturbations of unidirectional flows in two dimensions are the most unstable. As such, the existence of an unstable two dimensional solution provides a lower bound on the Reynold's number for the corresponding set of solutions which transform to the two dimensional problem. It is thus sufficient to consider only the two dimensional case, using the standard notation instead of the previously defined tilde notation.

We now define a new function which will encode both amplitudes of our two dimensional disturbance. The stream function ψ is defined for two dimensional incompressible flows as a function satisfying conversation of mass.[3] That is

$$\frac{\partial\psi}{\partial x}+\frac{\partial\psi}{\partial y}=0.$$

By making the following identification, it follows immediately from the smoothness of partials that ψ obeys the above equation.

$$\frac{\partial \psi}{\partial y} = u'_x, \tag{3.35}$$

$$\frac{\partial \psi}{\partial x} = -u'_y. \tag{3.36}$$

Given $\mathbf{u}'$ is some normal mode, the stream function can thus be expressed as the same exponential mode with some amplitude $\phi(y)$. The amplitudes of our perturbation are thus given by

$$\hat{u}_x = \frac{\partial \phi}{\partial y}, \tag{3.37}$$

$$\hat{u}_y = -i\alpha\phi. \tag{3.38}$$

Our goal now is to express our equations of motion for the perturbation amplitudes in terms of our stream function amplitude ϕ. Substituting our expressions for $\hat{\mathbf{u}}$ into (2.34) gives an expression for the pressure

$$\hat{p} = \frac{1}{i\alpha Re}\left(\frac{\partial^2}{\partial y^2} - \alpha^2 - i\alpha Re(U-c)\right)\frac{\partial \phi}{\partial y} + \frac{\partial u}{\partial y}\phi \tag{3.39}$$

with boundary conditions that $\hat{u}_x = \frac{\partial \phi}{\partial y} = \alpha\phi = i\hat{u}_y = 0$ at the boundaries of the channel, We then substitute this into (2.35) to obtain

$$\left[\frac{\partial^2}{\partial y^2} - \alpha^2 - i\alpha Re(U-c)\right](-i\alpha\phi) = Re\frac{\partial}{\partial y}\frac{1}{i\alpha Re}\left(\frac{\partial^2}{\partial y^2} - \alpha^2 - i\alpha Re(u-c)\right)\frac{\partial \phi}{\partial y} + \frac{\partial u}{\partial y}\phi. \tag{3.40}$$

Multiplying both sides by $i\alpha$ and evaluating derivatives yields the equation

$$\begin{aligned} \alpha^2\frac{\partial^2 \phi}{\partial y^2} - \alpha^4\phi - i\alpha^3 Re(u-c)\phi = \\ \left(\frac{\partial^4 \phi}{\partial y^4} - \alpha^2\frac{\partial^2 \phi}{\partial y^2} - i\alpha Re\left((u-c)\frac{\partial^2 \phi}{\partial y^2} + \frac{\partial \phi}{\partial y}\frac{\partial u}{\partial y}\right) + i\alpha Re\left(\frac{\partial \phi}{\partial y}\frac{\partial u}{\partial y} + \frac{\partial^2 u}{\partial y^2}\phi\right)\right). \end{aligned} \tag{3.41}$$

Cancelling like terms and moving terms with coefficients to one side yields the Orr-Sommerfeld Equation. We have the proven the following result.

Theorem 3.4.2 — The Orr-Sommerfeld Equation. A stream function mode $\psi = \phi e^{i(\alpha x - \alpha ct)}$ obeys the following equation

$$\left(\frac{\partial^2}{\partial y^2} - \alpha^2\right)^2\phi = i\alpha Re\left((u-c)\left(\frac{\partial^2}{\partial y^2} - \alpha^2\right)\phi - \frac{\partial^2 u}{\partial y^2}\phi\right) \tag{3.42}$$

with boundary conditions that $\frac{\partial \phi}{\partial y} = \alpha\phi = 0$ at the boundaries of the channel. This is stable if a permitted value of c has Im(c)$\leq$0.

This final equation involves our base flow u, our real parameters α and Re, a complex parameter c, and the stream function amplitude. As stated previously, the stability is entirely determined by the

sign of Im(c), but the flow itself, just still obey the local behavior of the Navier-Stokes Equations. This poses the problem of determining the behavior of c in terms of the other parameters. At least by inspection, this is no easy task: c is deeply embedded in the differential equation, and solving for it explicitly would do little to tell us about behavior of solutions involving c.

Considering solutions to the Orr-Sommerfeld equation requires a fair bit of theory from ordinary differential equations. Specifically, the Orr-Sommerfeld equation defines what is known as an eigenvalue problem. This means that the equation can be rewritten as a matrix equation of the form

$$A\mathbf{v} = \lambda\mathbf{v}, \tag{3.43}$$

where $\mathbf{v}$ is a vector of eigenfunctions. The eigenvalue λ in this case can be expressed in terms of our parameters α, c, and Re while our eigenvector is in terms of our stream function amplitude ϕ and its derivatives. From these solutions we may extrapolate the behavior of c, and thus the stability of the flow, in terms of α and Re. In general, eigenvalue problems are nontrivial to solve and the methods used for the Orr-Sommerfeld equation are beyond the scope of what is discussed in this chapter. The concluding section of this paper provides a qualitative interpretation of results for Couette and Poisseuille flow attributed to Schmid and Henningson. This will include a discussion of eigenspectra and marginal stability curves, and how these determine the critical Reynold's number.

4. The Variational Formulation

4.1 Introduction

> Whenever flexibility in the geometry is important and the power of the computer is needed not only to solve a system of equations, but also formulate and assemble the discrete approximation in the first space, the finite element method has something to contribute.
>
> *Gilbert Strang*
> *George Fix*

In our study of the Couette-Poiseuille flow, we have derived an analytical solution to the Reduced Momentum Equation, that being the Velocity Profile shown in Chapter 2. However, the Couette-Poiseuille flow is the simplest case that offers insight into more complex flow problems. In reality, it is impossible to find analytical solutions to complex flow problems because of complicated domain conditions and variable material composition. Even though there is technically no need to solve this problem numerically, the study of formulating and implementing the Finite Element Method for this simpler problem serves as an introduction for how engineers and mathematicians use this method to solve more complicated problems.

The Finite Element Method relies on the variational formulation ("weak formulation"), which is a reformulation of our original PDE ("strong form"). The original strong form may not be efficient, or even possible, to solve given the domain or material composition in question. Additionally, the continuity and differentiability of our field variables is higher in strong form, a stricter requirement. In our case, the strong form of our PDE requires the velocity u to have partial derivatives up to order two. These issues motivate the variational formulation.

The weak formulation "relaxes" the PDE. In other words, we make the weakest possible assumptions on the field variables involved to loosen the requirements/constraints on the field variables. In our case, we will see that our variational formulation lowers the partial differentiability requirement to first order. The strong form and weak form are equivalent in that one can reverse the

steps to get back to the strong form. The weak form, most importantly, constitutes a well-posed problem, which means that a small residual, or error in the output, signifies that the error in the input is small. In other words, the residual is a sufficient metric for measuring the error. This is due to the Lax-Milgram Theorem, which will all be elucidated later in this chapter. Although for most problems, weak solutions are not exact solutions, the reduction in the requirements makes the problem easier to solve and, nevertheless, yields very accurate solutions with mesh refinement.

In this chapter, we will proceed as follows:

1. Our derivation will include function spaces such as L^2 and H_0^1 so in this chapter, we will define these spaces and include physical motivations for using these spaces.
2. We will then introduce the notions of inner products and norms and provide proofs to the Poincaré inequality, Cauchy Schwartz inequality, and the inner product induced norm. This section will serve as an important toolbox in deriving our variational formulation.
3. We will derive our variational formulation for the Reduced Momentum Equation for Couette-Poiseuille flow.
4. We will prove the existence and uniqueness of the solution to the variational formulation using the Lax-Milgram Theorem.

At the conclusion of this chapter, the reader will be prepared to learn how the Finite Element Method handles this variational formulation with Couette-Poiseuille flow.

4.2 Physical Motivations Behind Use of Requisite Function Spaces

Recall the Reduced Momentum Equation for Couette-Poiseuille flow:

$$\mu \frac{\partial^2 u}{\partial y^2} = \frac{dp}{dx}.$$

As we discussed in the introduction, we need mathematical description of flows to hone insights. In flows in general, differences in local velocity exert variable forces on adjacent fluid particles, which alter the flow and the dissipating energy. For example, changes in velocity can cause one layer of fluid to exert a force or drag on an adjacent layer. The dissipating energy must be finite. Regard the formula for total kinetic energy

$$\text{Kinetic Energy} := \frac{1}{2}\rho \int_{-L}^{L} |u|^2 \, dy.$$

where ρ is the constant density of our incompressible fluid. Thus, in our first function space with which we will be working enforces this physical constraint; we restrict to velocity functions with finite total kinetic energy. Next, note that the patterns in fluid flow are in large part a result local changes in velocity, represented mathematically by velocity derivatives. Hence, the second function space with which we will be working also enforces this physical constraint; we restrict further to velocity functions whose first partial derivatives have finite total kinetic energy. The velocity is zero on boundary of domain $[-L, L]$ due to the no-slip condition. This is accurate when the boundary represents fixed solid walls that are not moving. A heuristic is described in *Introduction to the Numerical Analysis of Incompressible Viscous Flows* by William Layton [9].

4.3 Inner Products and Norms

Now that we have explored the corresponding mathematical constraints of finite energy, we will solidify key concepts from Linear Algebra and Functional Analysis that will serve us well in our derivation of the variational formulation. After laying the groundwork with the inner product and norm on a vector space, we will establish a link between the function spaces in which we will be

working and their inner products and norms. Then, we will encounter the Poincaré inequality and Cauchy-Schwartz inequality, which will prove to be useful tools in proving the equivalence of the norm and semi-norm on $H_0^1([-L,L])$ and aspects of the variational formulation derivation, which will be explained in further detail later in the chapter. Now, let us introduce the inner product.

Definition 4.3.1 Let V be a vector space. Then an **inner product** on V, denoted as $\langle\cdot,\cdot\rangle$, is an operation between two elements of V and mapping the result to a real number. The inner product satisfies:

1. Symmetry: $\langle u,v\rangle = \langle v,u\rangle \ \forall u,v \in V$.
2. Bilinearity: $\langle c_1 u + c_2 v, w\rangle = c_1\langle u,w\rangle + c_2\langle v,w\rangle$ and $\langle w, c_1 u + c_2 v\rangle = c_1\langle w,u\rangle + c_2\langle w,v\rangle \quad \forall u,v,w \in V$ and $\forall c_1,c_2 \in \mathbb{R}$.
3. Non-negativity: $\forall u \in V$, $\langle u,u\rangle \geq 0$ and equality holds if and only if $u = 0$.

A vector space together with a fixed inner product is called an inner product space, or a **Hilbert Space**.

Now that we have a way to define operations between vectors in vector spaces, we naturally desire to assign a length, or magnitude, to these elements. We introduce the norm, which assigning non-negative lengths to elements in V.

Definition 4.3.2 A **norm**, denoted as $\|\cdot\|$, is a real valued function defined on a vector space V,which satisfies the following properties:

1. Non-negativity: $\|u\| \geq 0$ and equality holds if and only if $u = 0$.
2. Homogeneity: $\|c\,u\| = |c|\,\|u\| \ \ \forall u \in V$ and $\forall c \in \mathbb{R}$.
3. Triangle Inequality: $\|u+w\| \leq \|u\| + \|w\| \quad \forall u,w \in V$

Since we require velocity functions to have finite total kinetic energy, it is very useful to have tools allowing us to, in essence, measure velocity functions. We will now introduce the Cauchy-Schwartz Inequality, which allows us to bound inner products. This will be a useful tool in the proof of the induced norm among other requisite proofs included in the variational formulation derivation.

Theorem 4.3.1 — The Cauchy-Schwartz Inequality. Let $u,v \in V$ where V is an inner product space and $\langle\cdot,\cdot\rangle_*$ is the inner product. Then

$$|\langle u,v\rangle_*| \leq \|u\|_*\,\|v\|_* \quad \forall u,v \in V.$$

Proof. Let $u,v \in V$ be arbitrary. For the sake of convenience, I will drop the asterick from the inner product and norm notation. Let us start with the trivial case when $\|u\|$ or $\|v\|$ are equal to 0. Then $|\langle u,v\rangle| = \|u\|\,\|v\|$, which directly follows from the non-negativity property of inner products, a trivial result. Now suppose u and v are not parallel, in particular, $\|u\|, \|v\| \neq 0$. There are two cases to consider:
If $\langle u,v\rangle = 0$, then u and v are orthogonal with respect to $\langle\cdot,\cdot\rangle$ and $|\langle u,v\rangle| < \|u\|\,\|v\|$, another trivial case.
If $\langle u,v\rangle \neq 0$, then suppose if $\forall\lambda \in \mathbb{R}\ \langle u+\lambda v, u+\lambda v\rangle > 0$ then $u+\lambda v \neq 0$ because if $u = -\lambda v$, then

$$\begin{aligned}
|\langle u,v\rangle| &= |\langle -\lambda v, v\rangle| \\
&= |\lambda|\,\langle v,v\rangle \\
&= |\lambda|\,\|v\|^2 \\
&= |\lambda|\,\|v\|\,\|v\| \\
&= \|u\|\,\|v\|
\end{aligned}$$

and the Cauchy-Schwartz Inequality holds. Now by bilinearity and symmetry, this inner product $\langle u+\lambda v, u+\lambda v\rangle > 0$ yields the following:

$$\begin{aligned}
0 &< \langle u+\lambda v, u+\lambda v\rangle \\
&= \langle u,u\rangle + \langle u,\lambda v\rangle + \langle \lambda v,u\rangle + |\lambda|^2 \langle v,v\rangle \\
&= \|u\|^2 + |\lambda|^2 \|v\|^2 + 2\langle u,\lambda v\rangle \\
&= \|u\|^2 + |\lambda|^2 \|v\|^2 + 2\lambda \langle u,v\rangle.
\end{aligned}$$

Now, let us set $\lambda = \langle u,v\rangle t$ where $t \in \mathbb{R}$ for a reason that will become apparent later in the proof. Note that u,v are fixed so $\langle u,v\rangle$ is also fixed at this point. There is a bijection between λ and t. That is, whatever we fix $\lambda \in \mathbb{R}$ to be, we can find a unique $t \in \mathbb{R}$ such that $\lambda = \langle u,v\rangle t$ by setting $t = \frac{\lambda}{\langle u,v\rangle}$. Now, for all $t \in \mathbb{R}$, we have

$$0 < \|u\|^2 + t^2 |\langle u,v\rangle|^2 \|v\|^2 + 2|\langle u,v\rangle|^2 t.$$

This is a real-valued polynomial in t of order 2 because the coefficient on t^2 is strictly positive. A second order real polynomial represents a parabola but our condition is that it is strictly positive. Thus, our polynomial cannot have real roots. In other words, the discriminant must be strictly negative. Let us consider the discriminant:

$$\begin{aligned}
0 &> (2|\langle u,v\rangle|^2)^2 - 4(\|v\|^2 |\langle u,v\rangle|^2)(\|u\|^2) \\
&= 4|\langle u,v\rangle|^4 - 4\|v\|^2 |\langle u,v\rangle|^2 \|u\|^2.
\end{aligned}$$

We divide by $4|\langle u,v\rangle| \neq 0$ to obtain

$$\begin{aligned}
|\langle u,v\rangle|^2 - \|v\|^2 \|u\|^2 < 0 \ \text{ which directly implies,} \\
|\langle u,v\rangle|^2 < \|v\|^2 \|u\|^2 \ \text{ or,} \\
|\langle u,v\rangle| < \|u\| \|v\|,
\end{aligned}$$

completing the proof.

■

Corollary 4.3.2 — The Triangle Inequality. Let $u,v \in V$ be arbitrary. Then $\|u+v\| \leq \|u\| + \|v\|$.

Proof. Let $u,v \in V$ be arbitrary and consider the following reasoning:

$$\begin{aligned}
\|u+v\|^2 &= \langle u+v,u+v\rangle, \\
&= \langle u,u\rangle + \langle v,v\rangle + 2\langle u,v\rangle, \\
&= \|u\|^2 + \|v\|^2 + 2\langle u,v\rangle, \\
&\leq \|u\|^2 + \|v\|^2 + 2\|u\|\|v\| \ \text{ by the Cauchy-Schwartz Inequality,} \\
&= (\|u\| + \|v\|)^2.
\end{aligned}$$

Thus, it follows $\|u+v\| \leq \|u\| + \|v\|$, completing our proof. ■

We now want to show that the inner product induces a norm on the space it is over. The Cauchy-Schwartz inequality is trivial in geometric interpretation, but is a very useful tool that helps us in our further derivations, and notably the triangle inequality, required in the proof of the induced norm.

Theorem 4.3.3 — Induced Norm. Let V be an inner product space with the inner product denoted as $\|u\| = \langle u,u\rangle$. Then $\sqrt{\langle u,u\rangle}$ defines a norm on V.

Proof. By bilinearity of inner products, for any $c \in \mathbb{R}$,

$$\begin{aligned}\|cu\| &= \sqrt{\langle cu, cu\rangle},\\ &= \sqrt{c^2\langle u,u\rangle},\\ &= |c|\,\|u\|.\end{aligned}$$

Additionally, it is clear that $\|u\| \geq 0$ and $\|u\| = 0$ if and only if $u = 0$, which follows from the properties of inner products (i.e. $\langle u,u\rangle \geq 0$ and equality holds if and only if $u = 0$). The Triangle Inequality requirement follows exactly from our previous proof of the Triangle Inequality, completing our proof. ■

Definition 4.3.3 We now define the space of square-integrable functions, $L^2([-L,L])$, on a domain $[-L,L] \subset \mathbb{R}$ as

$$L^2([-L,L]) = \{w : \int_{-L}^{L} w^2\,dy < \infty\}.$$

Proposition 4.3.4 $L^2([-L,L])$ is a Hilbert Space with the inner product

$$\langle u,w\rangle_{L^2} = \int_{-L}^{L} uw\,dy.$$

Proof. To prove symmetry, we want to show that $\langle u,v\rangle = \langle v,u\rangle\ \forall u,v \in L^2([-L,L])$. Fix $u,v \in L^2([-L,L])$. Since function multiplication is commutative,

$$\langle u,v\rangle = \int_{-L}^{L} uv\,dy = \int_{-L}^{L} vu\,dy = \langle v,u\rangle.$$

For bilinearity, we want to show $\forall \lambda_1,\lambda_2 \in \mathbb{R}$ and $\forall u,v,w \in L^2([-L,L])$ that

$$\begin{aligned}\langle \lambda_1 u + \lambda_2 w, v\rangle &= \lambda_1\langle u,v\rangle + \lambda_2\langle w,v\rangle,\\ \langle u, \lambda_1 w + \lambda_2 v\rangle &= \lambda_1\langle u,w\rangle + \lambda_2\langle u,v\rangle.\end{aligned}$$

Let $\lambda_1,\lambda_2 \in \mathbb{R}$ be arbitrary and $u,v,w \in L^2([-L,L])$. Then by linearity of integration,

$$\begin{aligned}\langle \lambda_1 u + \lambda_2 w, v\rangle &= \int_{-L}^{L} (\lambda_1 u + \lambda_2 w)\,v\,dy,\\ &= \lambda_1 \int_{-L}^{L} uv\,dy + \lambda_2 \int_{-L}^{L} wv\,dy,\\ &= \lambda_1\langle u,v\rangle + \lambda_2\langle w,v\rangle.\end{aligned}$$

We have shown that $\langle u,v\rangle$ is symmetric, so we may use symmetry to show

$$\langle u, \lambda_1 w + \lambda_2 v\rangle = \lambda_1\langle u,w\rangle + \lambda_2\langle u,v\rangle.$$

Since $\langle \lambda_1 u + \lambda_2 w, v\rangle = \langle v, \lambda_1 u + \lambda_2 w\rangle$ by symmetry, then

$$\begin{aligned}\langle v, \lambda_1 u + \lambda_2 w\rangle &= \lambda_1 \langle u, v\rangle + \lambda_2 \langle w, v\rangle, \\ &= \lambda_1 \langle v, u\rangle + \lambda_2 \langle v, w\rangle, \text{ by symmetry.}\end{aligned}$$

Lastly, for non-negativity, we want to show for all $u \in L^2([-L,L])$, $\langle u,u\rangle \geq 0$ and equality holds if and only if $u = 0$. Well, if $u \neq 0$, then $\langle u,u\rangle > 0$ and if $\langle u,u\rangle = 0$, then it follows that $u \equiv 0$ completing the proof. ■

It follows that an inner product always induces a norm so the $L^2([-L,L])$ norm is defined as

$$\|u\|_{L^2} = \left(\int_{-L}^{L} u^2\, dy\right)^{\frac{1}{2}}.$$

Although functions may be elements of $L^2([-L,L])$, we cannot assume, or even be sure that their derivatives or partial derivatives exist or all are elements of $L^2([-L,L])$. Our problem certainly contains derivatives and partial derivatives, so if we still hold the $L^2([-L,L])$ space as a pillar in our problem, we must create a subspace of $L^2([-L,L])$ with the added requirement that derivatives and partial derivatives of functions of $L^2([-L,L])$ exist and are also elements of $L^2([-L,L])$.

Definition 4.3.4 We define this exact space, namely the **Sobolev space of order 1**

$$H^1([-L,L]) = \{w : w \in L^2([-L,L]), \frac{\partial w}{\partial y} \in L^2([-L,L])\}$$

In our PDE, $u(L) = U$ and $u(-L) = 0$, but as we will see in our variational formulation derivation, we will need functions that vanish at the boundary.

Definition 4.3.5 Consequently, we define the closure of $H^1([-L,L])$, denoted as H_0^1, which is defined as

$$H_0^1([-L,L]) = \{w : w \in H^1([-L,L]), w(L) = w(-L) = 0\}.$$

We note that $H_0^1([-L,L])$ is also a Hilbert Space with the associated inner product

$$\langle u,w\rangle_{H_0^1([-L,L])} = \langle u,w\rangle_{L^2([-L,L])} + \left\langle \frac{\partial u}{\partial y}\frac{\partial w}{\partial y}\right\rangle_{L^2([-L,L])}.$$

Proof. To prove symmetry, we want to show that $\langle u,w\rangle = \langle w,u\rangle\ \forall u,w \in H_0^1([-L,L])$. Using the symmetry of the $L^2([-L,L])$ inner product, it follows that

$$\begin{aligned}\langle u,w\rangle_{H_0^1([-L,L])} &= \langle u,w\rangle_{L^2([-L,L])} + \left\langle \frac{\partial u}{\partial y}, \frac{\partial w}{\partial y}\right\rangle_{L^2([-L,L])}, \\ &= \langle w,u\rangle_{L^2([-L,L])} + \left\langle \frac{\partial w}{\partial y}, \frac{\partial u}{\partial y}\right\rangle_{L^2([-L,L])}, \\ &= \langle w,u\rangle_{H_0^1([-L,L])}.\end{aligned}$$

For bilinearity, we want to show $\forall \lambda_1, \lambda_2 \in \mathbb{R}$ and $\forall u,v,w \in H_0^1([-L,L])$ that

$$\begin{aligned}\langle \lambda_1 u + \lambda_2 w, v\rangle &= \lambda_1 \langle u,v\rangle + \lambda_2 \langle w,v\rangle \\ \langle u, \lambda_1 w + \lambda_2 v\rangle &= \lambda_1 \langle u,w\rangle + \lambda_2 \langle u,v\rangle.\end{aligned}$$

Let $\lambda_1, \lambda_2 \in \mathbb{R}$ be arbitrary and $u, v, w \in H_0^1([-L,L])$. Then

$$\begin{aligned}\langle \lambda_1 u + \lambda_2 w, v\rangle_{H_0^1([-L,L])} &= \langle \lambda_1 u + \lambda_2 w, v\rangle_{L^2([-L,L])} + \langle \lambda_1 \frac{\partial u}{\partial y} + \lambda_2 \frac{\partial w}{\partial y}, \frac{\partial v}{\partial y}\rangle_{L^2([-L,L])},\\ &= \lambda_1 \langle u, v\rangle_{L^2([-L,L])} + \lambda_2 \langle w, v\rangle_{L^2([-L,L])} + \lambda_1 \left\langle \frac{\partial u}{\partial y}, \frac{\partial v}{\partial y}\right\rangle_{L^2([-L,L])} + \lambda_2 \left\langle \frac{\partial w}{\partial y}, \frac{\partial v}{\partial y}\right\rangle_{L^2([-L,L])}\end{aligned}$$

by the bilinearity of the $L^2([-L,L])$ inner product. The above equation is equal to $\lambda_1 \langle u, v\rangle_{H_0^1([-L,L])} + \lambda_2 \langle w, v\rangle_{H_0^1([-L,L])}$. A similar argument shows that $\langle u, \lambda_1 w + \lambda_2 v\rangle = \lambda_1 \langle u, w\rangle + \lambda_2 \langle u, v\rangle$.

Lastly, for non-negativity, we want to show $\forall u \in H_0^1([-L,L])$, $\langle u, u\rangle \geq 0$ and equality holds if and only if $u = 0$. This directly follows from the non-negativity of the $L^2([-L,L])$ inner product, completing the proof. ■

Similarly, this inner product induces the $H_0^1([-L,L])$ norm denoted as follows:

$$\|w\|_{H_0^1([-L,L])} := \sqrt{\|w\|^2_{L^2([-L,L])} + \left\|\frac{\partial w}{\partial y}\right\|^2_{L^2([-L,L])}}.$$

Lastly, in our quest to elucidate the concept of the $H_0^1([-L,L])$ space, we will introduce the concept of the semi-norm on $H_0^1([-L,L])$, defined and denoted as

$$|w|_{H_0^1([-L,L])} := \left\|\frac{\partial w}{\partial y}\right\|_{L^2([-L,L])}.$$

The semi-norm is indeed a norm, except for the contingency that $|w|_{H_0^1([-L,L])}$ may not equal 0 when $w = 0$. Visually, the semi-norm is a "portion", or component of the overall norm. The semi-norm and norm discrepancy will prove to be useful in particular details of our derivation, namely the equivalence of the norm and semi-norm on $H_0^1([-L,L])$. In order to prove this result, we need the following inequality:

Theorem 4.3.5 — Poincaré inequality. Let $[-L,L]$ be a bounded set of $\mathbb{R}^n$; then there exists a constant C_L such that

$$\|w\|_{L^2([-L,L])} \leq C_L |w|_{H_0^1([-L,L])} \quad \forall w \in H_0^1([-L,L]).$$

The proof of this fundamental result is beyond the scope of this project,. However, detailed proofs can be found in *Numerical Models for Differential Problems*[13] by Alfio Quarteroni and *Introduction to the Numerical Analysis of Incompressible Viscous Flows* [9]. The Poincaré inequality serves as a tool in the proof of the equivalence of the norm and semi-norm on $H_0^1([-L,L])$.

Theorem 4.3.6 — Equivalence of norm and semi-norm on $H_0^1([-L,L.\ )]Thenorm\|w\|_{H_0^1([-L,L])}$ is equivalent to the semi-norm $|w|_{H_0^1([-L,L])}$, that is, there exists $c_1, c_2 > 0$ such that

$$c_1 |w|_{H_0^1([-L,L])} \leq \|w\|_{H_0^1([-L,L])} \leq c_2 |w|_{H_0^1([-L,L])}.$$

Proof. We begin by observing that

$$\begin{aligned}
\|w\|^2_{H^1_0([-L,L])} &= \|w\|^2_{L^2([-L,L])} + \left\|\frac{\partial w}{\partial y}\right\|^2_{L^2([-L,L])}, \\
&\geq 0 + \left\|\frac{\partial w}{\partial y}\right\|^2_{L^2([-L,L])}, \\
&= \left\|\frac{\partial w}{\partial y}\right\|^2_{L^2([-L,L])}, \\
&= |w|^2_{H^1_0([-L,L])}.
\end{aligned}$$

Next, by the Poincaré inequality, we know there exists a constant C_L such that

$$\|w\|_{L^2([-L,L])} \leq C_L\, |w|_{H^1_0([-L,L])} \quad \forall w \in H^1_0([-L,L]).$$

Then it follows that

$$\begin{aligned}
\|w\|^2_{H^1_0([-L,L])} &= \|w\|^2_{L^2([-L,L])} + |w|^2_{H^1_0([-L,L])}, \\
&\leq C_L^2\, |w|^2_{H^1_0([-L,L])} + |w|^2_{H^1_0([-L,L])}, \\
&= (C_L^2 + 1)\, |w|^2_{H^1_0([-L,L])},
\end{aligned}$$

where $C_L^2 + 1 > 0$, completing our proof. ■

We are now fully equipped to derive our variational formulation and prove it has a unique solution.

4.4 Variational Formulation

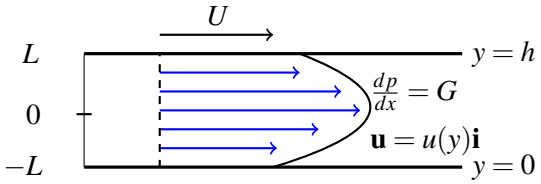

Figure 4.1: The domain $[-L,L]$ in question concerning our application of FEM on Couette-Poiseuille flow in a 2D channel of width h

.

Our derivation is motivated from similar derivations included in *Numerical Models for Differential Problems* [13] by Alfio Quarteroni. Recall our governing PDE:

$$\mu \frac{\partial^2 u}{\partial y^2} = \frac{dp}{dx}.$$

Define $\mathscr{F}(w) = \mu \frac{\partial^2 w}{\partial y^2} - \frac{dp}{dx}$. It follows that $\mathscr{F}(u) = 0$ for true solution u. Let $\widetilde{u}$ approximate the solution u and $e_u = u - \widetilde{u}$ is the error. Evidently, the lower the error, the better the approximation is to the true solution. The error is essential but very often unknowable because if we know the error and the approximate value, adding then gives the true value. If the true value were knowable, then there would be no reason to approximate in the first place. This motivates the **residual**, or error in the output, which we will define as

$$R(\widetilde{u}) = \mathscr{F}(u) - \mathscr{F}(\widetilde{u}) = -\mathscr{F}(\widetilde{u}).$$

We cannot always measure error in the input, but we can always measure the residual, as it is easily computable, and thus, observable. A sizable topic of study of numerical methods is centered around how the observable residual relates to the unknowable error. If a problem is ill-posed, then even though we may have a small residual, there can be a large error and then the residual is not a good metric to minimize the error. However, since our strong form is well posed, then a small residual corresponds to a small error. So our goal is to minimize the residual in our problem, or have $\|R(u)\|^2_{L^2([-L,L])} = 0$. Equivalently,

$$\langle R(u), R(u)\rangle = 0.$$

According to Riesz Representation Theorem, a focal theorem in Functional Analysis, if we consider an alternate equivalent problem and show $\langle R(u), w\rangle = 0$ for all $w \in H^1_0([-L,L])$, then $\|R(u)\|^2_{L^2([-L,L])} = 0$, which is exactly what we are looking for. Now we continue:

$$\begin{aligned} 0 &= \langle R(u), w\rangle \\ &= \int_{-L}^{L} R(u)\, w\, dy \\ &= \int_{-L}^{L} (-\mu \frac{\partial^2 u}{\partial y^2} + \frac{dp}{dx})\, w\, dy \\ &= -\mu \int_{-L}^{L} \frac{\partial^2 u}{\partial y^2}\, w\, dy + \int_{-L}^{L} \frac{dp}{dx}\, w\, dy \\ \mu \int_{-L}^{L} \frac{\partial^2 u}{\partial y^2}\, w\, dy &= \int_{-L}^{L} \frac{dp}{dx}\, w\, dy. \end{aligned}$$

This is equivalent to multiplying our Reduced Momentum Equation for Couette-Poiseuille Flow by a test function w and integrating on both sides:

$$\begin{aligned} \int_{-L}^{L} \mu \frac{\partial^2 u}{\partial y^2} w\, dy &= \int_{-L}^{L} \frac{dp}{dx} w\, dy, \\ \int_{-L}^{L} \mu \frac{\partial}{\partial y}\left(\frac{\partial u}{\partial y}\right) w\, dy &= \int_{-L}^{L} \frac{dp}{dx} w\, dy. \end{aligned}$$

In essence, we want to test our solution to our problem with all test functions in our test function space. Recall the integration by parts formula:

$$\int_{-L}^{L} f\, dg = f\, g\Big|_{-L}^{L} - \int_{-L}^{L} g\, df.$$

Set $f = w$ and $g = \frac{\partial u}{\partial y}$, then integrating by parts, we obtain

$$\begin{aligned} \mu\, w \frac{\partial u}{\partial y}\Big|_{-L}^{L} - \int_{-L}^{L} \mu \frac{\partial u}{\partial y}\frac{\partial w}{\partial y} dy &= \int_{-L}^{L} \frac{dp}{dx}\, w\, dy, \\ \mu(w(L)\frac{\partial u}{\partial y}(L) - w(-L)\frac{\partial u}{\partial y}(-L)) - \int_{-L}^{L} \mu \frac{\partial u}{\partial y}\frac{\partial w}{\partial y} dy &= \int_{-L}^{L} \frac{dp}{dx}\, w\, dy. \end{aligned}$$

In order to simplify the above equation, we want the test function space V to have the condition that $w(L) = w(-L) = 0$ so the above equation simplifies to

$$-\int_{-L}^{L} \mu \frac{\partial u}{\partial y}\frac{\partial w}{\partial y} dy = \int_{-L}^{L} \frac{dp}{dx}\, w\, dy.$$

As we continue, we will let $V = \{w \in H^1([-L,L]) : w(L) = w(-L) = 0\} = H_0^1([-L,L])$. However the solution space U is defined as $U = \{u \in H^1([-L,L]) : u(L) = U,\ u(-L) = 0\}$. We must point out that later, we will see that the fact that $V \neq U$ will slightly impede our progress in proving our variational formulation is well-posed. The Lax Milgram Theorem states that in order for our variational formulation to have a unique solution, we require that the test function space and solution space are the same. That is, we need $V = U$. We introduce the lift to solve this. In essence, we want to find a relationship that relates the homogenous problem to the nonhomogenous problem, and this difference is the lift function. A lift shifts boundary data and we want to lift the boundary data so the function spaces are the same. If u is the solution to the non-homogenous problem, let $\mathring{u} = u - R_u$ be the solution to the corresponding homogenous Dirichlet problem. We have $R_u = \frac{y+L}{2L}U$ as the lift function. Note that $R_u(-L) = \frac{-L+L}{2L}U = 0$ and $R_u(L) = \frac{L+L}{2L}U = U$. It follows

$$\mathring{u}(-L) = u(-L) - R_u(-L) = 0 - 0 = 0$$

and

$$\mathring{u}(L) = u(L) - R_u(L) = u(L) - U = U - U = 0.$$

Thus, $\mathring{u}$ is the solution to the homogenous problem. It follows that $u = \mathring{u} + R_u$. The use of the lift shifts the boundary data. If we substitute $\mathring{u} + R_u$ for u into our variational formulation, then our variational problem will be in terms of the solution to the homogenous problem:

$$\begin{aligned}
-\int_{-L}^{L} \mu \frac{\partial u}{\partial y}\frac{\partial w}{\partial y}dy &= \int_{-L}^{L} \frac{dp}{dx} w\, dy, \\
-\int_{-L}^{L} \mu \frac{\partial}{\partial y}(\mathring{u} + R_u)\frac{\partial w}{\partial y}dy &= \int_{-L}^{L} \frac{dp}{dx} w\, dy, \\
-\int_{-L}^{L} \mu \frac{\partial \mathring{u}}{\partial y}\frac{\partial w}{\partial y}dy - \int_{-L}^{L} \mu \frac{\partial R_u}{\partial y}\frac{\partial w}{\partial y}dy &= \int_{-L}^{L} \frac{dp}{dx} w\, dy, \\
-\int_{-L}^{L} \mu \frac{\partial \mathring{u}}{\partial y}\frac{\partial w}{\partial y}dy &= \int_{-L}^{L} \frac{dp}{dx} w\, dy + \int_{-L}^{L} \mu \frac{\partial R_u}{\partial y}\frac{\partial w}{\partial y}dy.
\end{aligned}$$

To proceed with our derivation, we have to consider the $\frac{\partial R_u}{\partial y}$ term:

$$\begin{aligned}
\frac{\partial R_u}{\partial y} &= \frac{\partial}{\partial y}(\frac{y+L}{2L}U), \\
&= \frac{\partial}{\partial y}(\frac{y}{2L}U + \frac{L}{2L}U), \\
&= \frac{U}{2L}.
\end{aligned}$$

Then we may proceed with the derivation:

$$\begin{aligned}
-\int_{-L}^{L} \mu \frac{\partial \mathring{u}}{\partial y}\frac{\partial w}{\partial y}dy &= \int_{-L}^{L} \frac{dp}{dx} w\, dy + \int_{-L}^{L} \mu \frac{\partial R_u}{\partial y}\frac{\partial w}{\partial y}dy, \\
&= \int_{-L}^{L} \frac{dp}{dx} w\, dy + \int_{-L}^{L} \mu (\frac{U}{2L})\frac{\partial w}{\partial y}dy, \\
&= \int_{-L}^{L} \frac{dp}{dx} w\, dy + \frac{\mu U}{2L}\int_{-L}^{L} \frac{\partial w}{\partial y}dy, \\
&= \int_{-L}^{L} \frac{dp}{dx} w\, dy + \frac{\mu U}{2L}(w(L) - w(-L)), \\
&= \int_{-L}^{L} \frac{dp}{dx} w\, dy.
\end{aligned}$$

Thus, solving the nonhomogenous problem is the same as solving the homogenous problem, except the solution only differs by the linear lifting factor R_u. We are tasked with solving

$$\int_{-L}^{L} \mu \frac{\partial \mathring{u}}{\partial y} \frac{\partial w}{\partial y} dy = -\int_{-L}^{L} \frac{dp}{dx} w\, dy$$

for all $w \in H_0^1([-L,L])$. Let $a(\mathring{u},w) := \int_{-L}^{L} \mu \frac{\partial \mathring{u}}{\partial y} \frac{\partial w}{\partial y} dy$ where $\mathring{u} = u - R_u = u - \frac{y+L}{2L} U$ and $F(w) := -\int_{-L}^{L} \frac{dp}{dx} w\, dy$ where F is a **functional**, or operator on a vector space, which assigns a real number to each element of V.

Definition 4.4.1 — Homogenous Dirichlet Problem. Our problem is now to find $\mathring{u} \in H_0^1([-L,L])$ such that $a(\mathring{u},w) = F(w)\ \forall w \in H_0^1([-L,L])$.

However, there is one critical component that is missing: We do not know that a solution $\mathring{u}$ exists and, if it did, if it is unique. Nonetheless, if

1. We show there exists a unique $\mathring{u}$ in the corresponding homogenous problem and
2. solving our non-homogenous problem and the corresponding homogenous problem is the same, except that the solution u to the non-homogenous problem differs by a linear factor, that is, $u = \mathring{u} + \frac{y+L}{2L} U$.

Then, we may conclude that u is the unique solution to the corresponding non-homogenous problem. That is, there exists a unique $u \in U = \{u \in H^1([-L,L]) : u(L) = U,\ u(-L) = 0\}$ such that

$$a(u,w) = F(w)\ \forall w \in H_0^1([-L,L]),$$

where $a(u,w) = \int_{-L}^{L} \mu \frac{\partial u}{\partial y} \frac{\partial w}{\partial y} dy$ and $F(w) = -\int_{-L}^{L} \frac{dp}{dx} w\, dy$ and $\mathring{u} = u - R_u = u - \frac{y+L}{2L} U$. Thus, our last task now is to show that there exists a unique $\mathring{u}$, which we will prove by the Lax-Milgram Theorem in the next section.

4.5 Existence and Uniqueness of the Solution

A natural following question would be centered around the existence and uniqueness of a solution to this weak formulation, to which the Lax-Milgram Theorem speaks directly.

Lax-Milgram Theorem Given a Hilbert Space $(H,(\cdot,\cdot))$, a continuous, coercive bilinear form $a(\cdot,\cdot)$ and a continuous linear functional $F \in H'$, there exists a unique $u \in H$ such that

$$a(u,v) = F(v) \quad \forall v \in H.$$

Lax-Milgram asserts that a weak formulation of an elliptic problem is well-posed. The proof of this powerful result hinges on the advanced result from Functional Analysis called Riesz Representation Theorem. A proof can be found on pages $60-61$ of *The Mathematical Theory of Finite Element Methods* by Brenner and Scott. In order to invoke the Lax Milgram Theorem on the corresponding homogenous variational formulation, we must show that $a(u,w)$ is symmetric, bilinear, coercive, and continuous while our functional $F(w)$ is linear and bounded.

Proposition 4.5.1 A form $a(\cdot,\cdot)$ is

1. symmetric if $a(u,w) = a(w,u)\ \forall u,w \in H_0^1([-L,L])$,
2. bilinear if $\forall \lambda_1, \lambda_2 \in \mathbb{R}$ and $\forall u,v,w \in H_0^1([-L,L])$ that

$$a(\lambda_1 u + \lambda_2 w, v) = \lambda_1 a(u,v) + \lambda_2 a(w,v)$$
$$a(u, \lambda_1 w + \lambda_2 v) = \lambda_1 a(u,w) + \lambda_2 a(u,v),$$

3. coercive if $\exists\, c > 0$ such that

$$a(u,u) \geq c \|u\|^2_{H_0^1([-L,L])}\ \ \forall u \in H_0^1([-L,L]),$$

4. continuous if there exists $M > 0$ such that

$$|a(u,w)| \leq M \|u\|_{H_0^1([-L,L])} \|w\|_{H_0^1([-L,L])} \quad \forall u,w \in H_0^1([-L,L]).$$

Proof. To prove symmetry, fix $u,w \in H_0^1([-L,L])$. Since function multiplication is commutative,

$$a(u,w) = \int_{-L}^{L} \mu \frac{\partial u}{\partial y}\frac{\partial w}{\partial y} dy = \int_{-L}^{L} \mu \frac{\partial w}{\partial y}\frac{\partial u}{\partial y} dy = a(w,u).$$

To show bilinearity, let $\lambda_1, \lambda_2 \in \mathbb{R}$ be arbitrary and $u,v,w \in H_0^1([-L,L])$. Then

$$\begin{aligned} a(\lambda_1 u + \lambda_2 w, v) &= \int_{-L}^{L} \mu \frac{\partial}{\partial y}(\lambda_1 u + \lambda_2 w)\frac{\partial v}{\partial y} dy \\ &= \int_{-L}^{L} \mu (\lambda_1 \frac{\partial u}{\partial y} + \lambda_2 \frac{\partial w}{\partial y})\frac{\partial v}{\partial y} dy \\ &= \lambda_1 \int_{-L}^{L} \mu \frac{\partial u}{\partial y}\frac{\partial v}{\partial y} dy + \lambda_2 \int_{-L}^{L} \mu \frac{\partial w}{\partial y}\frac{\partial v}{\partial y} dy \\ &= \lambda_1 a(u,v) + \lambda_2 a(w,v). \end{aligned}$$

We have shown that $a(u,v)$ is symmetric, so we may use symmetry to show

$$a(u, \lambda_1 w + \lambda_2 v) = \lambda_1 a(u,w) + \lambda_2 a(u,v).$$

Since $a(\lambda_1 u + \lambda_2 w, v) = a(v, \lambda_1 u + \lambda_2 w)$ by symmetry, then

$$\begin{aligned} a(v, \lambda_1 u + \lambda_2 w) &= \lambda_1 a(u,v) + \lambda_2 a(w,v) \\ &= \lambda_1 a(v,u) + \lambda_2 a(v,w), \text{ by symmetry.} \end{aligned}$$

To prove coercivity, let $u \in H_0^1([-L,L])$ be arbitrary. Then

$$\begin{aligned} a(u,u) &= \mu \int_{-L}^{L} (\frac{\partial u}{\partial y})^2 dy, \\ &= \mu \left\| \frac{\partial u}{\partial y} \right\|_{L^2}^2 \quad (\text{since } \|u\|_{L^2} = (\int_{-L}^{L} u^2 dy)^{\frac{1}{2}}), \\ &= \mu \, |u|_{H_0^1([-L,L])}^2 \quad (\text{definition of the semi-norm on } H_0^1([-L,L])), \\ &\geq \mu c \, \|u\|_{H_0^1([-L,L])} \quad (\text{for some } c > 0), \end{aligned}$$

the last step following from the equivalence of the norm and semi-norm on $H_0^1([-L,L])$.

Now we want to show continuity of our form. First, due to the equivalence of the norm and semi-norm on $H_0^1([-L,L])$, there exists $c > 0$ such that

$$|v|_{H_0^1([-L,L])} \leq c \, \|v\|_{H_0^1([-L,L])} \quad \forall v \in H_0^1([-L,L])$$

Now, consider $|a(u,w)|$:

$$\begin{aligned} |a(u,w)| &= \mu \left| \langle \frac{\partial u}{\partial y}, \frac{\partial w}{\partial y} \rangle_{L^2} \right|, \\ &= \mu \left| \int_{-L}^{L} \frac{\partial u}{\partial y}, \frac{\partial w}{\partial y} dy \right| \quad (\text{definition of } L^2 \text{ inner product}), \\ &\leq \mu \left\| \frac{\partial u}{\partial y} \right\|_{L^2} \left\| \frac{\partial w}{\partial y} \right\|_{L^2} \quad (\text{by the Generalized Cauchy-Schwartz Inequality}), \\ &= \mu \, |u|_{H_0^1([-L,L])} \, |w|_{H_0^1([-L,L])} \quad (\text{definition of the semi-norm on } H_0^1([-L,L])), \\ &\leq \mu \, c^2 \, \|u\|_{H_0^1([-L,L])} \, \|w\|_{H_0^1([-L,L])} \quad (\text{for some } \ c > 0), \end{aligned}$$

the last step following from the equivalence of the norm and semi-norm on $H_0^1([-L,L])$. That is, $\exists\, c > 0$ such that

$$|v|_{H_0^1([-L,L])} \leq c\,\|v\|_{H_0^1([-L,L])} \quad \forall v \in H_0^1([-L,L]).$$

Then let $M = \mu\, c^2$, completing our proof. ■

Now that we have proven that our form is bilinear, symmetric, coercive, and continuous, we must place certain restrictions on our functional F, requiring it to be linear and bounded.

Proposition 4.5.2 A functional F is linear if

$$F(\lambda_1 u + \lambda_2 w) = \lambda_1 F(u) + \lambda_2 F(w) \quad \forall u, w \in H_0^1([-L,L]), \forall \lambda_1, \lambda_2 \in \mathbb{R}$$

and bounded if $\exists C > 0$ such that

$$|F(w)| \leq C\,\|w\|_{H_0^1([-L,L])} \quad \forall w \in H_0^1([-L,L]).$$

Proof. This is a straight forward proof. Let $\lambda_1, \lambda_2 \in \mathbb{R}$ and $u, w \in H_0^1([-L,L])$ be arbitrary. Then

$$\begin{aligned}
F(\lambda_1 u + \lambda_2 w) &= -\int_{-L}^{L} \frac{dp}{dx}\,(\lambda_1 u + \lambda_2 w)\,dy \\
&= -\int_{-L}^{L} (\lambda_1 \frac{dp}{dx}\,u + \lambda_2 \frac{dp}{dx} w)\,dy \\
&= -\lambda_1 \int_{-L}^{L} \frac{dp}{dx}\,u\,dy - \lambda_2 \int_{-L}^{L} \frac{dp}{dx}\,w\,dy \\
&= \lambda_1 (-\int_{-L}^{L} \frac{dp}{dx}\,u\,dy) + \lambda_2 (-\int_{-L}^{L} \frac{dp}{dx}\,w\,dy) \\
&= \lambda_1 F(u) + \lambda_2 F(w).
\end{aligned}$$

Now to show our functional is bounded, first, recall from Chapter 2 that the applied pressure gradient $\frac{dp}{dx} = 0$ if the flow is Plane Couette and $\frac{dp}{dx} = G > 0$ if the flow is Plane Poiseuille. We will naturally proceed considering both cases. Let $w \in H_0^1([-L,L])$ be arbitrary.
If $\frac{dp}{dx} = 0$, then

$$\begin{aligned}
|F(w)| &= \left| \int_{-L}^{L} 0\,w\,dy \right|, \\
&= \left| \int_{-L}^{L} 0\,dy \right|, \\
&= 0, \\
&\leq C\,\|w\|_{H_0^1([-L,L])}
\end{aligned}$$

$\forall C > 0$ since $\|w\|_{H_0^1([-L,L])} \geq 0 \forall w \in H_0^1([-L,L])$. If $\frac{dp}{dx} = G > 0$, then

$$\begin{aligned}
|F(w)| &= \left| \int_{-L}^{L} G\,w\,dy \right|, \\
&= |\langle G, w \rangle_{L^2}| \quad \text{(by the definition of the } L^2 \text{ inner product)}, \\
&\leq \|G\|_{L^2}\,\|w\|_{L^2} \quad \text{(by the Generalized Cauchy-Schwartz Inequality)}, \\
&= |G|\,\|w\|_{L^2}, \\
&\leq |G|\,C_p\,|w|_{H_0^1([-L,L])} \quad \text{(for some } C_p > 0 \text{ constant by the Poincaré inequality)}, \\
&\leq |G|\,C_p\,c\,\|w\|_{H_0^1([-L,L])} \quad \text{(for some } c > 0),
\end{aligned}$$

the last step following from the equivalence of the norm and semi-norm on $H_0^1([-L,L])$. Then let $C = |G|C_p\,c$, completing the proof. ■

Since we have shown that $a(\cdot,\cdot)$ is symmetric, bilinear, coercive, and continuous while our functional F is linear and bounded, we can invoke the Lax Milgram Theorem on the homogenous problem and state that there exists a unique $\mathring{u} \in H_0^1([-L,L])$ such that

$$a(\mathring{u},w) = F(w)\ \forall w \in H_0^1([-L,L]).$$

Consider what we have just shown:

1. We invoked the Lax-Milgram Theorem to show there exists a unique $\mathring{u}$ in the corresponding homogenous problem.
2. Solving our non-homogenous problem and the corresponding homogenous problem is the same, except that the solution u to the non-homogenous problem differs by a linear factor, that is, $u = \mathring{u} + \frac{y+L}{2L}U$.

Definition 4.5.1 Thus, we may conclude that u is the unique solution to the corresponding non-homogenous problem. That is, there exists a unique $u \in U = \{u \in H^1([-L,L]) : u(L) = U,\ u(-L) = 0\}$ such that

$$a(u,w) = F(w)\ \forall w \in H_0^1([-L,L]),$$

where $a(u,w) = \int_{-L}^{L} \mu \frac{\partial u}{\partial y}\frac{\partial w}{\partial y}dy$ and $F(w) = -\int_{-L}^{L} \frac{dp}{dx}\,w\,dy$ and $\mathring{u} = u - R_u = u - \frac{y+L}{2L}U$ is the solution to the homogenous problem.

Our variational formulation problem is well-posed and now we are prepared to learn in the next chapter how the Finite Element Method handles this well-posed variational formulation.

5. The Finite Element Method

I have had my results for a long time: but I do not yet know how I am to arrive at them

Carl Friedrich Gauss

5.1 The Weak Formulation and Motivation

We begin this chapter with a recap from the previous chapter in regards to the weak formulation displayed below. The question we may have at this point is: why do we need a weak formulation and how is it relevant for the Finite Element Method? Why do we need the Finite Element Method in the first place?

$$a(u,w) = \int_{-L}^{L} \mu \frac{\partial u}{\partial y} \frac{\partial w}{\partial y} dy$$

$$F(u) = \int_{-L}^{L} \frac{dP}{dx} w dy$$

In essence, solving the strong form is not always the easiest or most efficient path to find classical solutions to a particular problem. Furthermore, incorporating boundary conditions is difficult when solving for strong forms directly because the continuity requirement is much stronger. Thus, in order to find a path of least resistance, weak formulations are preferred over the strong formulation. They reduce the continuity requirements on the basis functions functions which allows us to use and implement nth-degree polynomials as we see fit (In this chapter we will be mainly working with linear and quadratic Lagrange polynomials). With the weak formulation, Neumann boundary conditions come naturally and hence, implementing them
It is important to note that the weak formulation rarely (if at all) gives exact solutions because of

the reduction in the requirements of smoothness and weak implementation of Neumann boundary and Dirichlet conditions. We are, in essence, approximating the solution to the approximation of the true solution. Additionally, the Weak formulation still gives relatively very accurate results with the mesh refinement, which are extremely good in the applied sciences. More importantly, utilizing the FEM allows us to obtain a more than decent approximation of our true solution in a finite dimensional subspace without actually knowing what the true solution looks like. Improving the accuracy of a solution in weak formulations depend upon the type of problem you are solving. The accuracy can be improved by using higher-order degree functions.

Thus we restate definition 4.5.1 and as our starting point, we have the following:
There exists a unique $u \in U = \{u \in H^1([-L,L]) : u(L) = U,\ u(-L) = 0\}$ such that

$$a(u,w) = F(w)\ \forall w \in H_0^1([-L,L]),$$

where $a(u,w) = \int_{-L}^{L} \mu \frac{\partial u}{\partial y}\frac{\partial w}{\partial y} dy$ and $F(w) = -\int_{-L}^{L} \frac{dp}{dx} w\, dy$ and $\mathring{u} = u - R_u = u - \frac{y+L}{2L}U$ is the solution to the homogeneous problem.

The following sections will be based on the statement above and we will eventually utilize the weak formulation for FEM and find solutions for the Plane Couette and Poiseuille flows

5.2 Understanding the Basics

In this chapter we will explore a basic idea: Have an approximation of simple functions under different sub-domains for the Couette, Poiseuille flows. In essence, in the Finite Element Method (FEM) we are given a domain that is divided into finite elements or subdomains. The advantages of this technique allows us to represent a complicated function as a collection of simple polynomials (citation: J.N. Reddy). This is given that the function and possibly derivatives up to a specific order are continuous at the connecting points.

Throughout this chapter we will follow a similar strategy outlined in Reddy's An introduction to Finite Element Methods to solve the Couette, Poiseauille and Couette-Poiseauille flows. Our strategy is as follows:

1. Divide the domain, Ω, into parts in order to represent the geometry and solution of the problem at hand
2. Over each subdomain, seek an approximation to the solution of linear combinations of nodal values and functions, and derive the algebraic relations among the nodal values of the solutions over each subdomain.
3. Once all parts have been solved, we assemble them to obtain the solution

Before we proceed to employ our strategy for the different flows, let's discuss further what we results we should expect to find when applying the FEM to each of the flows.

From the previous chapter, we can safely assume that we have a well-posed problem with a unique solution over the domain H_0^1. In essence we have to complete the following steps:

1. Basis functions ψ_i
2. Approximate $a(u,w) = \sum c_i(u)\psi_i(w)$
3. Determine the coefficient c_i

Finite element space for the model problem. When we look for a finite element solution in a finite dimensional space V^h, it should be a subspace of $H_0^1(-L,L)$ for a finite element method. For example, given a mesh for the 1D model, we can define a finite dimensional space using piecewise

continuous linear functions over the mesh. Now, $V^h = \{v^h \in H^1([-L,L]) : v(L) = 0,\ v(-L) = 0\}$ where v^h is continuous piecewise linear. The finite element solution would be chosen from the finite dimensional space Vh, a subspace of $H_0^1(-L,L)$. If the solution of the weak form is in $H_0^1(-L,L)$ but not in the V^h space; then an error is introduced on replacing the solution space with the finite dimensional space. Nevertheless, the finite element solution is the best approximation in V^h.

5.3 Properties, Boundary Conditions and Cea's Lemma

As pointed out in our previous section, we should expect to have our answer in the following form $\sum_{i=1}^{N+1} c_i(u)\psi_i(w)$ which we'll denote as matrix K with elements $c_{ij} = c(u)$. One important property that we will explore in this section is that we have a matrix K that is positive definite - a symmetric matrix with all positive eigenvalues. Such property in general makes it easier to choose the most convenient family of spaces, which from a computational point of view, requires a more than mild amount of computational power. Consider the following Theorem:
Theorem[section]

Theorem 5.3.1 *(Positive Definite)* The Matrix K associated to the discretization of an elliptic problem with the Galerkin Method is positive definite

Proof. Recall that a matrix $K \in \mathbb{R}^{n\times n}$ is said to be positive definite if

$$v^T K v \geqslant 0 \quad \forall v \in \mathbb{R}^n$$
$$v^T K v = 0 \iff v = 0$$

where $v = v_i \in \mathbb{R}^n \leftrightarrow v_h = \sum_{j=1}^{N_h} v_j\psi_j \in V_h$. Note that V_h is a family of spaces that depends on a positive parameter. Given that in the previous chapter we proved the bilinear and coercive form of $a(\cdot,\cdot)$, we have the following:

$$v^T K v = \sum_{j=1}^{N_h}\sum_{i=1}^{N_h} v_i a_{ij} v_j = \sum_{j=1}^{N_h}\sum_{i=1}^{N_h} v_i a(\psi_j,\psi_i) v_j$$
$$= \sum_{j=1}^{N_h}\sum_{i=1}^{N_h} a(v_i\psi_j, \psi_i v_j) = a(\sum_{j=1}^{N_h} v_j\psi_j, \sum_{i=1}^{N_h} v_i\psi_i)$$
$$= a(v_h,u_h) \geqslant \alpha||v_h||_V^2 \geqslant 0$$

■

Boundary conditions: For the Dirichlet condition, we have a specified value of the unknown potential on our boundary. Implementing this boundary condition simply requires setting all nodal values of the potential on the boundary to the given value, and only interior nodes in the problem are unknowns. For Neumann's condition, we have a specified value of the normal derivative of the potential on our boundary. This condition can be implemented by adding additional equations at the boundary which require boundary nodal values to be equal to the nearest interior neighbor in the direction of the respective normal vector we are working with.

More importantly Céa's lemma, Introduced by Jean Céa in his Ph.D. dissertation,is an important tool for proving error estimates for the finite element method applied to elliptic partial differential equations (citation: Layton ch.2). Cea's Lemma allows to find a unique solution to our problem under a certain domain Ω

Cea's Lemma: Suppose $a(\cdot,\cdot) : X \times X \mapsto \mathbb{R}$ is a continuous and coercive bilinear form and $F : X \mapsto \mathbb{R}$ is a bounded linear functional. Let $X^h \subset X$ be a finite dimensional subspace of X. Then, there exists a unique $u_h \in X_h$ satisfying

$$a(u_h, w_h) = F(w_h)$$

for all $w_h \in X_h$. The error $u - u_h$ satisfies

$$||u - u_h||_X \leqslant (1 + \tfrac{a_1}{a_0})\ inf_{w \in X_h}\ ||u - u_h||_X$$

The proof for Cea's Lemma can be found in William Layton's Introduction to the Numerical Analysis of Incompressible Viscous Flows

5.4 Working with the Weak Formulation

Recall from the previous chapter that we are introduced with the derivation and the general weak formulation that we will need in this section. Given our boundary conditions consider the following bilinear and linear forms:

$$a(u,w) = \int_{-L}^{L} \mu \frac{\partial u}{\partial y}\frac{\partial w}{\partial y} dy$$

$$F(u) = \int_{-L}^{L} \frac{dP}{dx} w dy$$

We will construct a matrix equation of the form $[K^e]c^e = F^e$. This is what we'll call a finite element model; the resulting algebraic equations will contain more unknowns than the number of algebraic equations. The coefficient matrix $[K^e]$ which is symmetric can be evaluated for a given element and data.

For a mesh of linear elements, the element Ω_e is located between the local nodes $x_a (= x_e = -L)$ and $x_b (= x_{e+1} = L)$.

Thus consider the following expressions:

$$K^e_{ij} = \int_{-L}^{L} \mu \frac{\partial u}{\partial y}\frac{\partial w}{\partial y} dy = \int_{x_e}^{x_{e+1}} \mu \frac{\partial \psi_i}{\partial y}\frac{\partial \psi_j}{\partial y} dy$$

$$f^e_i = \int_{-L}^{L} \frac{dP}{dx} w dy = \int_{x_e}^{x_{e+1}} \frac{dP}{dx} \psi^e_i dy = \int_{x_e}^{x_{e+1}} f_e \psi^e_i dy$$

or, in the local coordinate system $\tilde{y}$, where $y = y^e_1 + \tilde{y}$. This implies that $dy = d\tilde{y}$ and $\frac{d\psi^e_i}{dy} = \frac{d\psi^e_i}{\tilde{y}}$. This way we have $\psi^e_1(\tilde{y}) = 1 - \frac{\tilde{y}}{h_e}$ and $\psi^e_2(\tilde{y}) = \frac{\tilde{y}}{h_e}$. Thus our weak formulation becomes:

$$K^e_{ij} = \int_{-L}^{L} \mu \frac{\partial u}{\partial y}\frac{\partial w}{\partial y} dy = \int_{x_e}^{x_{e+1}} \mu \frac{\partial \psi_i}{\partial y}\frac{\partial \psi_j}{\partial y} dy = \int_{0}^{h_e} \mu \frac{\partial \psi_i}{\partial \tilde{y}}\frac{\partial \psi_j}{\partial \tilde{y}} dy$$

$$f^e_i = \int_{-L}^{L} \frac{dP}{dy} w dy = \int_{x_e}^{x_{e+1}} \frac{dP}{dy} \psi^e_i dy = \int_{0}^{h_e} \frac{dP}{d\tilde{y}} \psi^e_i dy$$

Now, we are ready to compute K_{ij}^e and f_i^e by our evaluating our integrals. Thus, we have:

$$K_{11}^e = \int_0^{h_e} \mu \frac{\partial \psi_i}{\partial \tilde{y}} \frac{\partial \psi_j}{\partial \tilde{y}} dy = \int_0^{h_e} \mu (\frac{-1}{h_e})(\frac{-1}{h_e}) d\tilde{y} = \frac{\mu}{h_e}$$

$$K_{12}^e = \int_0^{h_e} \mu (\frac{-1}{h_e})(\frac{1}{h_e}) d\tilde{y} = \frac{-\mu}{h_e} = K_{21}^e$$

$$K_{12}^e = \int_0^{h_e} \mu (\frac{1}{h_e})(\frac{1}{h_e}) d\tilde{y} = \frac{\mu}{h_e}$$

We can similarly compute the corresponding integrals for f_1^e, f_2^e:

$$f_1^e = \int_0^{h_e} f_e (1 - \frac{\tilde{y}}{h_e}) d\tilde{y} = \frac{1}{2} f_e h_e$$

$$f_2^e = \int_0^{h_e} f_e (\frac{\tilde{y}}{h_e}) d\tilde{y} = \frac{1}{2} f_e h_e$$

Thus our coefficient matrix and our column vector (f^e) are:

$$[K^e] = \frac{\mu_e}{h_e} \begin{bmatrix} 1 & -1 \\ -1 & 1 \end{bmatrix}$$

$$[f^e] = \frac{\mu_e h_e}{2} \begin{bmatrix} 1 \\ -1 \end{bmatrix}$$

In summary the element matrices for a our linear element is:

$$\frac{\mu_e}{h_e} \begin{bmatrix} 1 & -1 \\ -1 & 1 \end{bmatrix} \begin{bmatrix} u_1^e \\ u_2^e \end{bmatrix} = \frac{f_e h_e}{2} \begin{bmatrix} 1 \\ -1 \end{bmatrix} + \begin{bmatrix} Q_1^e \\ Q_2^e \end{bmatrix}$$

In a similar manner, for a mesh of quadratic elements, element Ω_e is located between the nodes $x_a (= x_{2e+1} = -L)$ and $x_b (= x_{2e+1} = L)$, hence similar to our previous procedure we have:

$$K_{ij}^e = \int_{-L}^{L} \mu \frac{\partial u}{\partial y} \frac{\partial w}{\partial y} dy = \int_{x_{2e-1}}^{x_{2e+1}} \mu \frac{\partial \psi_i}{\partial y} \frac{\partial \psi_j}{\partial y} dy$$

$$f_i^e = \int_{-L}^{L} \frac{dP}{dy} w dy = \int_{x_{2e-1}}^{x_{2e+1}} \frac{dP}{dy} \psi_i^e dy = \int_{x_{2e-1}}^{x_{2e+1}} f_e \psi_i^e dy$$

Before proceeding to evaluating the corresponding integrals for K^e and f^e, we consider the following general form for quadratic Lagrange interpolation function:

$$\psi_i^e = \frac{1}{D^e} (\alpha_i^e + \beta_1^e y + \omega_1^e y^2)$$

where D^e denotes the determinant of the matrix and $\alpha_i^e, \beta_1^e y, \omega_1^e y^2$ are the local nodal coordinates. When the second node, ψ_2^e, is placed at distance $\tilde{y} = \alpha_e$, where $\alpha = \frac{1}{2}$ for node 2, the quadratic

interpolation functions are:

$$\psi_1^e(\tilde{y}) = (1-\frac{\tilde{y}}{h})(1-\frac{2\tilde{y}}{h})$$
$$\psi_2^e(\tilde{y}) = 4\frac{\tilde{y}}{h}(1-\frac{\tilde{y}}{h})$$
$$\psi_3^e(\tilde{y}) = -\frac{\tilde{y}}{h}(1-\frac{2\tilde{y}}{h})$$

Now, evaluating the integrals with our quadratic interpolation functions we have:

$$K_{11} = \int_0^{h_e} \mu_e(\frac{-3}{h_e}+\frac{4\tilde{y}}{h_e^2})(\frac{-3}{h_e}+\frac{4\tilde{y}}{h_e^2})d\tilde{y} = \frac{7\mu_e}{3h_e}$$

$$K_{12} = \int_0^{h_e} \mu_e(\frac{-3}{h_e}+\frac{4\tilde{y}}{h_e^2})(\frac{4}{h_e}-\frac{8\tilde{y}}{h_e^2})d\tilde{y} = \frac{-8\mu_e}{3h_e} = K_{21}$$

$$K_{22} = \int_0^{h_e} \mu_e(\frac{4}{h_e}-\frac{8\tilde{y}}{h_e^2})(\frac{4}{h_e}-\frac{8\tilde{y}}{h_e^2})d\tilde{y} = \frac{7\mu_e}{3h_e}$$

Similarly for f_i^e we have the following:

$$f_1^e = \int_0^{h_e} f^e[1-\frac{3\tilde{y}}{h_e}+2(\frac{\tilde{y}}{h_e})^2]d\tilde{y} - \frac{f_e}{6h_e} = f_3^e$$

$$f_2^e = \int_0^{h_e} f^e[4\frac{\tilde{y}}{h_e}(1-\frac{\tilde{y}}{h_e})]d\tilde{y} = \frac{2f_e}{3h_e}.$$

Thus the element matrices of the quadratic element are:

$$\frac{\mu_e}{3h_e}\begin{bmatrix} 7 & -8 & 1 \\ -8 & 16 & -8 \\ 1 & -8 & 7 \end{bmatrix}\begin{bmatrix} u_1^e \\ u_2^e \\ u_3^e \end{bmatrix} = \frac{f_e h_e}{6}\begin{bmatrix} 1 \\ 4 \\ 1 \end{bmatrix} + \begin{bmatrix} Q_1^e \\ Q_2^e \\ Q_3^e \end{bmatrix}$$

Now that we have the simplest cases of element matrices for both the linear and quadratic elements, we are prepared to tackle

5.5 Couette and Poiseuille Flows

As introduced in the initial chapters, the Couette flow - a case of parallel flow, only one velocity component is different from 0 resulting in all the fluid moving in one direction. Thus the conservation of mass in this case is $\frac{\partial u}{\partial x} = 0$, this means that we'll have $u = u(y)$. This points to our momentum equation having the following form:

$$\mu\frac{\partial^2 u}{\partial y^2} = \frac{du}{dx}$$

Following similar techniques found in the previous section, we have the following finite element model for this special case:

$$[K^e][c^e] = f^e + [Q^e]$$

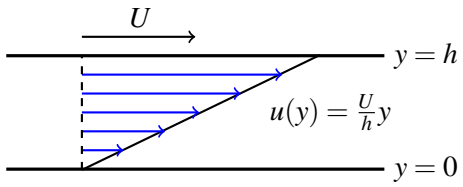

Figure 5.1: Couette flow in a 2D channel of width h

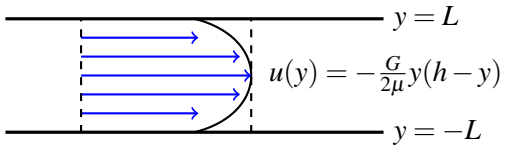

Figure 5.2: Poiseuille flow in a 2D channel of width $2L$

where

$$K_{ij}^e = \int_{-L}^{L} \mu \frac{\partial \psi_i}{\partial y} \frac{\partial \psi_j}{\partial y} dy$$

$$f_i^e = \int_{x_e}^{x_{e+1}} \frac{dP}{dx} \psi_i^e dy$$

$$Q_1^e = -(\mu \frac{du}{dy})_a$$

$$Q_2^e = -(\mu \frac{du}{dy})_b$$

Consider parallel flow between two long walls separated by a distance $2L$. We wish to determine the velocity $u(y)$ where $y \in [-L, L]$, for a given pressure gradient - dP/dx using our FEM. Consider the simplest element matrix case for the Couette Flow; a two element mesh of linear elements (where $h = L$). Performing similar techniques seen in the previous section we have the following element matrix:

$$\frac{\mu}{h} \begin{bmatrix} 1 & -1 & 0 \\ -1 & 2 & -1 \\ 0 & -1 & 1 \end{bmatrix} \begin{bmatrix} U_1^e \\ U_2^e \\ U_3^e \end{bmatrix} = \frac{q_0 h_e}{2} \begin{bmatrix} 1 \\ 4 \\ 1 \end{bmatrix} + \begin{bmatrix} Q_1^e \\ Q_2^e \\ Q_3^e \end{bmatrix}$$

Furthermore we consider the following boundary conditions:

$$\begin{aligned} Boundary \quad condition1 \quad &: u(-L) = u(L) = 0 \\ Boundary \quad condition2: \quad &u(-L) = 0, u(L) = U_0 \end{aligned}$$

Following the problem solving technique in the previous section we obtain the following results for the set of boundary condition 1:

$$U_2 = \frac{q_0 L^2}{2\mu}$$

Similarly for the set of boundary condition 2, we obtain the following result:

$$U_2 = \frac{q_0 L^2}{2\mu} + \frac{U_0}{2}$$

Now for the quadratic element case, where $h = 2L$ and following the same procedure as highlighted from the previous we obtain the following matrix:

$$\frac{\mu}{h}\begin{bmatrix} 7 & -8 & 1 \\ -8 & 16 & -8 \\ 1 & -8 & 7 \end{bmatrix}\begin{bmatrix} U_1^e \\ U_2^e \\ U_3^e \end{bmatrix} = \frac{q_0 L}{3}\begin{bmatrix} 1 \\ 4 \\ 1 \end{bmatrix} + \begin{bmatrix} Q_1^e \\ 0 \\ Q_3^e \end{bmatrix}$$

The solution for the quadratic mesh turns out to be the same as the linear mesh that is for boundary condition 1:

$$U_2 = \frac{q_0 L^2}{2\mu}$$

similarly for boundary condition 2:

$$U_2 = \frac{q_0 L^2}{2\mu} + \frac{U_0}{2}$$

6. Conclusion

Here, we present a comprehensive analysis of the hydrodynamic stability of plane Couette and plane Poiseuille flow. Although laminar flows are easy to describe analytically, turbulent flows are much more complex, making flow transition and stability a critical question in fluid dynamics. The Orr-Sommerfeld equation sets up an eigenvalue problem to determine fluid stability, and applying the Orr-Sommerfeld equation to simpler physical scenarios as provided by plane Couette and Poiseuille flows enables an understanding of how these mathematical tools might be used to comprehend more complex real-life problems.

Analytical results to the Orr-Sommerfeld equation for plane Couette and plane Poiseuille flow have been obtained and published ubiquitously [14]. As discussed in Chapter 3, the Orr-Sommerfeld equation poses an eigenvalue problem, meaning that it yields a finite set of discrete eigenvalues when solved for particular values of α, β, and Re. These finite eigenvalues can be visualized using eigenvalue spectra, where eigenvalues are plotted on the $c_i - c_r$ plane. The stability of a particular flow can be intuited by the clustering of eigenvalues along the branches of the figure pictured below and the sign of c_i, the imaginary component of the perturbation phase speed [14]. As evidenced by the figure below, plane Couette flow exhibits close clustering of its eigenvalues along the branches of the spectra, which indicates its stability for $Re = 1000$. On the contrary, the eigenvalues for plane Poiseuille flow are widely distributed along the left branch of the spectrum. In addition, one of the eigenvalues changes sign for c_i. Taken together, these observations lead to the conclusion that plane Poiseuille flow is not stable for $Re = 10000$, which means that a critical Re exists beyond which plane Poiseuille flow is not stable.

In order to find a critical Reynold's number for both of these flows, we may plot the contours of constant c_i in the $\alpha - Re$ plane, seeking the curve of marginal stability, that is where $c_i = 0$. This curve is the boundary between regions of stable flow, that is $c_i < 0$ and unstable flow where $c_i > 0$. Additionally, the minimum value of Re lying on the marginal curve defines the critical Reynold's number of the flow; any flow with a Reynold's number above this value may have a mode with an unstable value of c. Below we see the contours of constant c_i for Couette flow and Poiseuille flow. In the case of Couette flow, note that as α and Re approach large values, the contours seem to

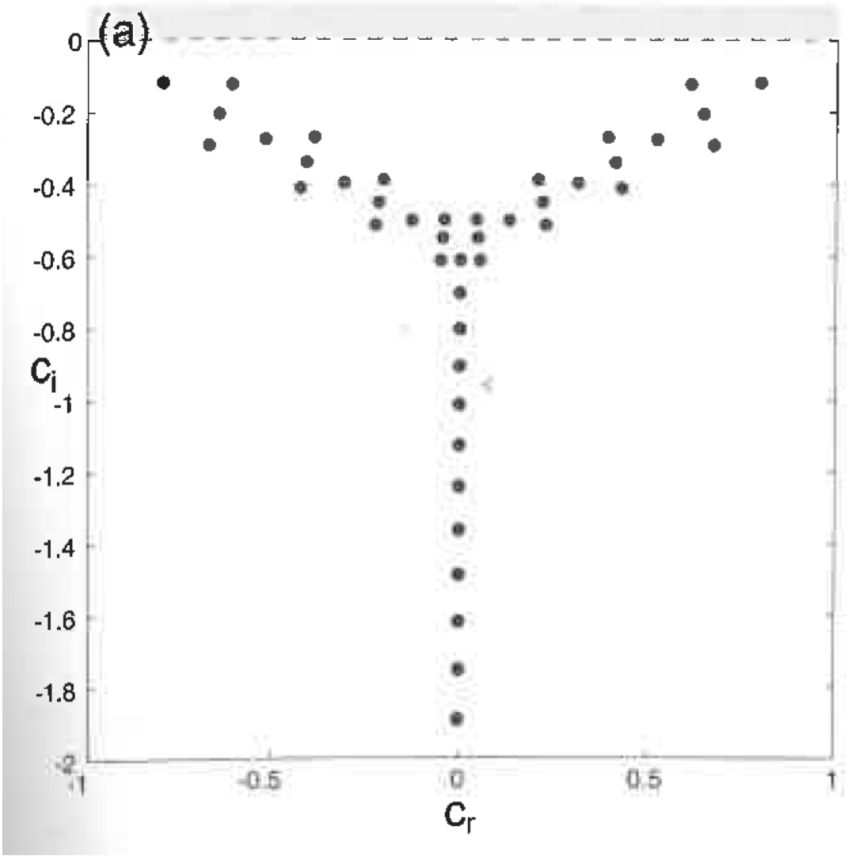

Figure 6.1: Spectra for plane Couette flow; $\alpha = 1$, $\beta = 1$, $Re = 1000$

flatten out, while maintaining a negative sign. This aligns with the result that Couette flow is stable at all Reynold's numbers [14]: c_i never changes sign, so no region of the plane is unstable. Even if a region was unstable, the curve of marginal stability would approach the α-axis, making the critical Reynold's number arbitrarily small.

However, Poiseuille flow presents a different set of contours. Most notably, there does exist a contour with $c_i = 0$, with the unstable region bounded by this curve shaded in the figure. We see that the contour does in fact have an extrema at roughly $Re = 6000$. This is the critical Reynold's number for plane Poiseuille flow. Above this value, there always exist modes with α values permitting unstable values of c, and thus making the whole perturbation unstable. One can extrapolate the two results given here to combined Couette-Poiseuille flow, where the motion of the top plate has a stabilizing effect on the unstable pressure driven flow. In fact, it has been shown that this flow become totally stable when the motion of the top plate is roughly 70 percent of the maximum pressure driven velocity [4].

We can show for various physical problems that the methods we used are applicable since they all lead to the same type of Partial differential equation and boundary condition and together are referred to as the strong form of the problem. We also showed that this so called strong form could be reformulated into an equivalent weak form. We emphasize that the weak form is the one on which the FEM approach is based. The reason is that the order of differentiation of the unknown is lower in the weak form than in the strong form, thus facilitating the approximation process. The weak form applies without changes to continuous as well as discontinuous problems, implying the important conclusion that the FE method also holds for continuous as well as discontinuous

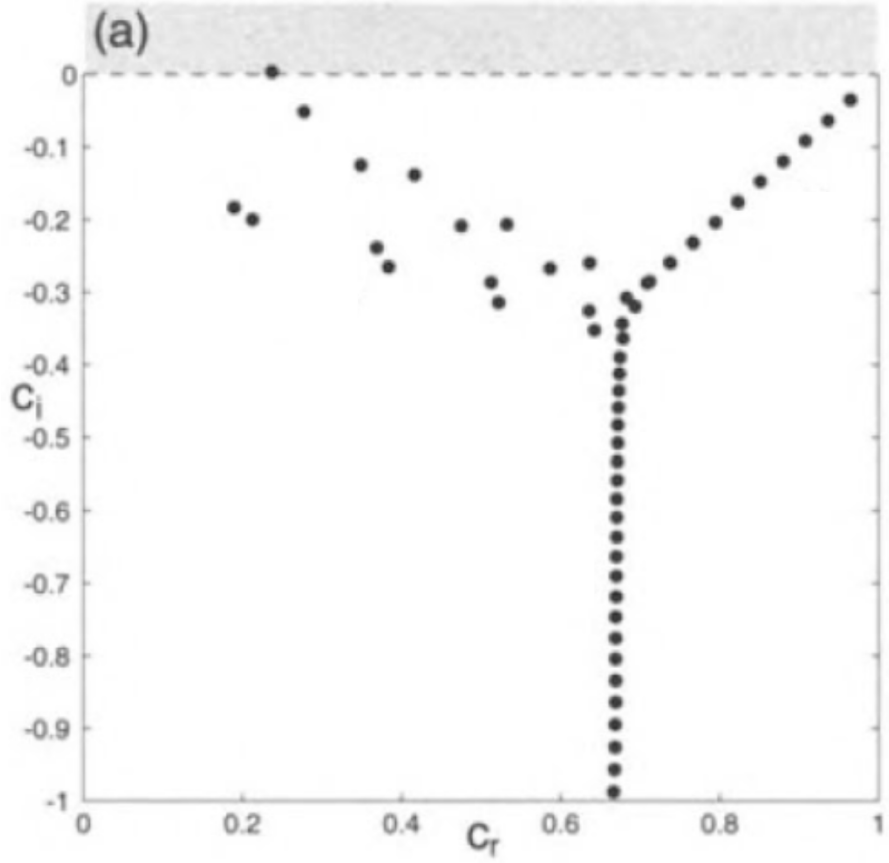

Figure 6.2: Spectra for plane Poiseuille flow; $\alpha = 1$, $\beta = 0$, $Re = 10000$

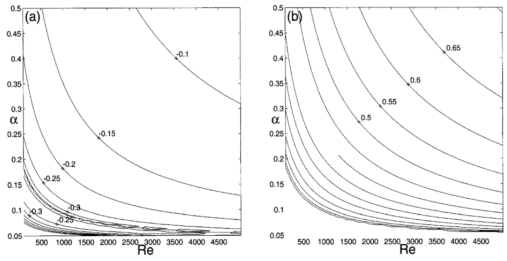

Figure 6.3: Curves for plane Couette flow with constant c_i (a) and c_r (b)

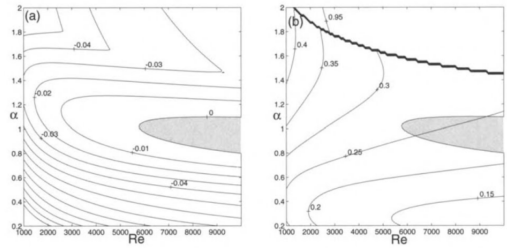

Figure 6.4: Curves for plane Poiseuille flow with constant c_i (a) and c_r (b)

problems. With our initial motivation to construct a weak formulation we went through several processes to make sure we paved the way for a method that exists and holds the property of unique-

ness under local subdomains. Although the FEM in itself is a very powerful tool to find relatively accurate solutions, there are other tools that are equally relevant and useful to solve similar type of problems. In our case we are referring to the Finite Volume Method. The basic principle includes the discretization and construction of control volumes for vertex centered schemes.

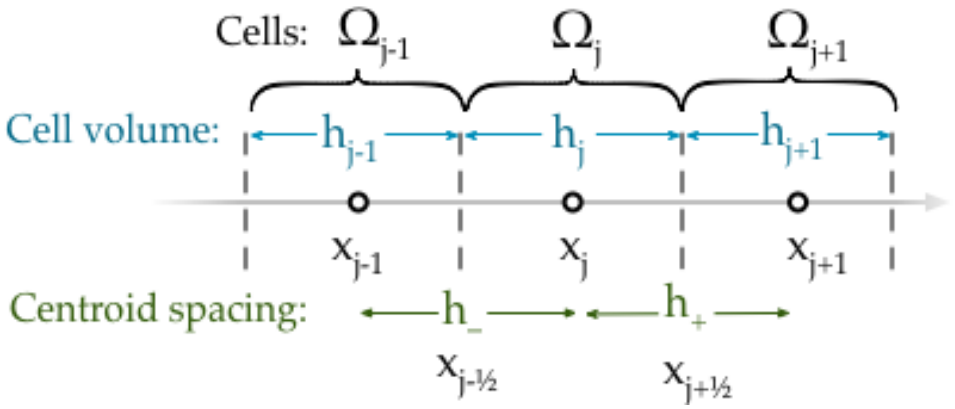

Figure 6.5: 1D Finite Volume Mesh with fixed minimum spacing

A brief description found in Quarteroni's Numerical Models for differential equations, provides a general but concise overview of what this method. In essence, in the finite volume method, the governing equations are integrated over a volume or cell assuming a piece-wise linear variation of the dependent variables (u, v, w, p, T). Again the piece-wise linear variation determines both the accuracy and the complexity. Using these integrations, you essentially balance fluxes across the boundaries of the individual volumes. The flux is calculated at the mid-point between the discrete nodes in the domain. Hence, you must calculate a flux between all neighboring nodes in the domain. In a topologically regular mesh (same number of divisions in any one direction), this flux calculation is quite straightforward. In an 'irregular' mesh (essentially non-rectangular) , this calculation will lead to an excruciating amount of fluxes and a major effort to make sure all the fluxes have been calculated properly.

Bibliography

[1] J. Anderson. *Computational Fluid Dynamics: The Basics with Applications*. McGraw Hill Education (India), 1995.

[2] G.K. Batchelor. Flow of a Uniform Incompressible Fluid. In *An Introduction to Fluid Dynamics*. Cambridge University Press, 1967.

[3] P. Kundu, I. Cohen, and D. Dowling. *Fluid Mechanics*. Elsevier.

[4] P.G. Drazin and W.H. Reid. Parallel Shear Flows. In *Hydrodynamic Stability*. Cambridge University Press, 1981.

[5] L.C. Evans. *Partial Differential Equations*, volume 19. American Mathematical Society, 2 edition.

[6] J. Gersting and D. Jankowski. Numerical methods for orr-sommerfeld problems. *International Journal for Numerical Methods in Engineering*, 4, 1972.

[7] M. Mathur, N.A. Jajal, and R.K. Singh. Finite Difference Solver for Couette Flow with Applied Pressure Gradients. January 2017.

[8] F. Lam. On Exact Solutions of the Navier-Stokes Equations for Unidirectional Flows. *arXiv*, 2015.

[9] W. Layton. *Introduction to the Numerical Analysis of Incompressible Viscous Fluids*. Society for Industrial and Applied Mathematics, 2008.

[10] MathWorks. MATLAB. Version R2017a. https://www.mathworks.com.

[11] J. Oliver and P. Howell. Viscous Flow: Lecture Notes. *Oxford University*, 2016.

[12] M.C. Potter. Stability of Plane Couette–Poiseuille Flow. 24(3):609–619, 1996.

[13] A. Quarteroni. *Numerical Models for Differential Problems*. Springer, 2009.

[14] P.J. Schmid and D.S Henningson. *Stability and Transition in Shear Flows*. Springer Science: Business Media, 2012.

[15] H.B. Squire. On the stability for three-dimensional disturbances of viscous fluid flow between parallel walls.

[16] D.B. Thapa and K.N. Uprety. Analytical and Numerical Solutions of Couette Flow Problem: A Comparative Study. *Journal of the Institute of Engineering*, June 2016.

[17] G.E. Urroz. Numerical Solution to Unsteady Two-Dimensional Poiseuille Flow. 4, November 2004.

[18] Wolfram. MATHEMATICA. Version 11. https://www.wolfram.com/mathematica/.